

SHRP-C-662

Concrete Microscopy

D.M. Roy
M.W. Grutzeck
B.E. Scheetz

Materials Research Laboratory
The Pennsylvania State University
University Park, Pennsylvania

G.M. Idorn
Neils Thaulow
K.T. Andersen

G.M. Idorn Consult A/S
Blokken 44 Birkerød
Denmark



Strategic Highway Research Program
National Research Council
Washington, DC 1993

SHRP-C-662
Contract C-201

Program Manager: *Don M. Harriott*
Project Manager: *Inam Jawed*
Production Editor: *Marsha Barrett*
Program Area Secretary: *Ann Saccomano*

June 1993

key words:
cement
concrete
fluorescence
microscopy
microstructure
sample preparation
thin section

Strategic Highway Research Program
National Academy of Sciences
2101 Constitution Avenue N.W.
Washington, DC 20418

(202) 334-3774

The publication of this report does not necessarily indicate approval or endorsement of the findings, opinions, conclusions, or recommendations either inferred or specifically expressed herein by the National Academy of Sciences, the United States Government, or the American Association of State Highway and Transportation Officials or its member states.

© 1993 National Academy of Sciences

Acknowledgments

The research described herein was supported by the Strategic Highway Research Program (SHRP). SHRP is a unit of the National Research Council that was authorized by section 128 of the Surface Transportation and Uniform Relocation Assistance Act of 1987.

Contents

Acknowledgments	iii
Abstract	vii
1 Introduction	1
Background	1
2 Preparation of Fluorescent, Concrete Thin-Sections	3
Instrumentation	5
Examination of Fluorescent Thin-Sections	8
References	11
3 Examination of SHRP 1-19 Concrete Samples	13
Introduction	13
Samples	13
Microstructural Data	14
Stereological Measurements	15
General Examination	16
Alternate Methods	19
References	20
4 Discussion	21
References	22
Appendix A Figures	23
Appendix B Tables	77
Appendix C Nordtest 677-87 Concrete, Hardened; Water-Cement Ratio	101

Abstract

Concrete microstructure can be evaluated using both thin and polished sections. Methods described in this report were developed as a supplement to ASTM 856 procedures. The use of an epoxy resin containing a fluorescent dye tended to enhance the ability to view porosity and mechanical features such as interface porosity and cracking. Relationships of formulation and microstructure for a series of nineteen concrete samples are presented (SHRP S89-1 to S89-19). The proposed methods are useful to the highway engineer on a variety of levels. A less skilled operator can use the epoxy impregnation technique for developmental and forensic purposes, to more easily observe effects of making and formulation on homogeneity, and the relationship of cracking and secondary hydration products in deteriorated concrete, respectively. The determination of water/cement ratio is more difficult inasmuch as it is done visually by comparing the fluorescence intensity of the unknown with a series of known standards.

Executive Summary

Optical and electron microscopy are valuable research tools for the study of concrete microstructure. ASTM-C-856 already has a standard practice in place giving details of how to use optical techniques for examination of hardened concrete. The supplemental methods described in the accompanying report were also used to examine hardened concrete specimens, S89-1 to S89-19. Although most of the report emphasizes data obtained using epoxy impregnated thin sections, alternate methods have also been explored (polished impregnated samples were examined in reflected fluorescent light and in the SEM).

Either thin sections or polished sections of concrete impregnated with an epoxy dye reveal enhanced inherent porosity of the paste, interface porosity and effects of cracking. In addition, water/cement (w/c) ratio can be determined by comparing paste porosity with a series of carefully prepared standard samples.

Impregnation is achieved using a combination of thin epoxy mixed with a fluorescent dye. The sample is evacuated with a vacuum pump for ~2 hours after which the epoxy is allowed to wet the sample and fill the pores/cracks. After the epoxy hardens one can either polish the sample for reflected light and SEM examination or prepare a ~20 μm thick thin section for transmitted light examination. Whereas the reflected light sample may be easier to make, it transmits light through translucent grains in the sample. The thin section sample is harder to make but it is more satisfactory for w/c determination because a uniform thickness thin sectioning results in uniformity and reproducibility of the amount of transmitted light.

Concrete microstructure is quite variable, and at least qualitatively, it can be correlated with the nature of the starting materials and the original formulation of the concrete. For example, a formulation with a higher w/c ratio than a companion concrete revealed a higher porosity in thin section and higher relief in polished section (the higher w/c matrix was just not as strong).

The examination of concrete microstructure, whether in thin section or reflected light/SEM, is a powerful one, useful to the highway engineer on a number of levels. For forensic purposes, it can be used to actually see why a concrete has deteriorated. In terms of developing a new concrete formulation or mixing procedure, the method can give the engineer information on homogeneity, relationship of porosity to interfacial characteristics, overall crack development, etc. These are easy to evaluate and do not require much more

training than that currently described in ASTM-C-856. However, on a more sophisticated level, the determination of w/c ratio is much more difficult. In this instance, the investigator must compare the fluorescence of known standards with that of the unknown.

1

Introduction

ASTM C 856 details a standard practice for petrographic examination of hardened concrete. It contains sections detailing microscopic methods to be used to examine polished sections and thin sections. It is a useful technique but one which is learned over long periods of time and examination of many specimens. ASTM states: "It is assumed that the examination will be made by persons qualified to operate the equipment used and to record and interpret the results obtained."

The methods and examples presented in the following report are a refinement of Romer's original work on fluorescent impregnation microscopy, and are directly related to the objectives of ASTM C 856. Fluorescent microscopy is a method by which the investigator is aided in his examination procedure by the impregnation of pores and voids by a fluorescent epoxy. When viewed under fluorescent light, features such as porosity and cracks are enhanced by the fluorescence of the dye used to impregnate the sample.

Proponents of the method include Bert Romer (Switzerland), Hollis Walker (USA) and Gunnar Idorn (Denmark). The following report was prepared with the cooperation of GMIC. The report is divided into three sections. The first deals with the method itself, i.e., the preparation of fluorescent thin sections, the equipment required, and some of the basic principles needed to examine the thin section. The second section of the report describes the results of using various methods to study a series of concrete specimens prepared in this study (SHRP 1-19). The final section is a discussion section giving both pros and cons of the method as a potential tool for the highway engineer.

Background

Thin sections have been used by petrographers and petrologists to study rocks for more than 150 years. One of the major advantages of this method, is that it provides an opportunity to both identify the individual mineral constituents and at the same time study their mutual interrelationships (fabric), their morphology and their amounts.

Not surprisingly, the use of petrographic thin-sections has gained increasing recognition within the field of concrete petrography. The first concrete thin-sections were hand-made and generally quite large, having a uniform thickness falling between 0.02-0.03 mm (20-30

microns). Thin-sectioning techniques have been improved, and several laboratories now manufacture thin sections of the desired thickness on automatic lapping machines (Ahmed, 1983).

Another major step forward was the introduction of the fluorescent impregnation method (Wilk et al., 1974) by which concrete is impregnated with a fluorescent epoxy prior to grinding. By excitation of the fluorescent epoxy in the concrete with ultra-violet or blue light, it became possible to observe even very small porosities and defects in the concrete (Walker and Marshall, 1979; Walker, 1979; Gudmundson et al., 1981; Wilk and Dubrolubov, 1984; Anderson and Thaulow, 1990).

The fluorescence method was further refined when it was demonstrated that it is possible to obtain reasonably accurate figures for the water-cement ratio used in the concrete (Walker's early work), by visual estimation of the brightness of the hardened cement paste when viewed in fluorescent light. This method was refined and quantified by Thaulow et al., 1982 and Damgaard Jensen, 1983. It is now a standard practice in several European countries to determine the w/c ratio of hardened concrete using fluorescent thin-sections. In addition, the preparation of fluorescent thin-sections has recently been approved as a Nordic test method, by Denmark, Norway, Sweden, Finland and Iceland (Nordtest 677-87, "Concrete, Hardened; Water-Cement Ratio," see Appendix C).

Today, about 6000-7000 fluorescent concrete thin-sections are prepared annually in Denmark alone for use in quality control, damage analyses and research. Practically none of these thin-sections are prepared solely for the determination of the water-cement ratio of the cement paste since the determination of the w/c ratio only represents a small part of the information which can be obtained from the study of fluorescent concrete thin-sections (Damgaard Jensen, 1985; Soers, 1985; Thaulow et al., 1989). For detailed evaluations of the method see Walker, 1979, and Mayfield, 1990. Both give statistics for fluorescent microscopy examination of thin and reflected light samples, respectively.

2

Preparation of Fluorescent Concrete Thin-Sections

Most of the equipment required for the preparation of thin-sections from concrete, is similar to the instrumentation used in the preparation of ordinary petrographic thin-sections. A large variety of brands, including self-made machinery, are currently used in the USA and Europe for the preparation of thin-sections. Consequently, a detailed description of these items is beyond the scope of this report. Interested readers are referred to ASTM C 856 or other publications dealing with thin-section preparation. However, these lists must be supplemented with a few additional items in order to ensure the optimum quality of the fluorescent thin-sections. These items include:

- A desiccator with an attached vacuum pump,
- A diamond grinding wheel (15-20 μm diamonds),
- An epoxy resin, preferably low viscosity, and
- Fluorescent dye.

Before preparation of the thin-section, it is important to select a proper volume of concrete for the thin-sectioning.

This selection should depend both on the representativeness of the cores/samples, and on the features which are being examined. If surface cracking and carbonation are to be investigated, it would be logical to thin-section exposed surfaces of the concrete. The identification of alkali-silica reactions and reacting aggregate particles usually requires that the thin-section be located a couple of centimeters away from the exposed surface of the concrete as general experience shows that these reactions tend to be weaker at the near-surface regions of the concrete.

The chosen area should be included in a rectangular piece of concrete, normally with the size: 45×30×20 mm, which is cut from the specimen with a rock saw. The cutting should be done with care in order to avoid the introduction of fine cracking and other flaws in the specimen.

The cut concrete specimen is then immersed in pure ethanol and allowed to reside there for approximately 12 hours. The ethanol replaces some of the water in the concrete which reduces the tendency of cracking in the concrete during the subsequent drying procedure.

The concrete specimen is then placed in a vacuum chamber equipped with a hot plate for final drying. It is important that this drying occurs at 30°-35°C (85°-95°F) as excessive heating will introduce undesirable microcracking in the specimen.

The specimen should be allowed to dry for approximately 2 hours.

The specimen is then placed in a small vessel, with the side to be mounted on the glass slide facing downwards, ready for the first vacuum impregnation with epoxy.

The epoxy should be of a low viscosity type in order to promote the penetration of the epoxy into the concrete. Likewise, the epoxy must be intermixed with precisely 1.1% by weight of a fluorescent dye. However, this may vary from epoxy to epoxy and dye to dye depending on the combination chosen by the investigator.

It is very important that the dosage of dye per volume of epoxy is accurately measured as even small variations in the concentration will seriously affect the determination of the w/c ratios on the finished thin-sections.

For the same reasons, one should ensure that the epoxy/dye mixture is completely homogenized. It is thus common practice to stir the mixture with a magnetic stirrer for at least 24 hours before use.

Once ready for use, the epoxy is poured into the small vessel, containing the specimen. The vessel is subsequently placed in a vacuum chamber and the specimen is allowed to soak at < 0.1 mbar pressure for 1 hour while the samples are still submerged in epoxy, air is then allowed to re-enter the chamber.

The penetration depth of the epoxy depends largely on the viscosity of the epoxy used and on the permeability of the concrete. It is normally observed that the concrete will be impregnated to a depth of approximately 1-2 mm. High strength concretes with a low w/c ratio and concretes with mineral admixtures such as silica fume are normally more difficult to impregnate adequately.

Following impregnation, the side opposite to the selected large face of the specimen is glued to a glass plate with an ultraviolet (UV) hardening glue.

The glass plate should be of appropriate size so that it fits the clamping device of the grinding equipment.

The next step is to prepare the selected face of the concrete specimen for mounting on the object glass.

The epoxy covering the exposed large face of the concrete specimen is carefully removed by mounting the glass plate which was glued to the specimen in the petrographic lapping machine and subsequently grinding the opposite face carefully in order to obtain a completely level surface. The finishing operation should be performed on a 15-20 μm diamond disc.

It is important that loose abrasives are never used during these operations as the grit tend to stick to the impregnating epoxy in the concrete. It must also be emphasized that the final operations of the grinding procedure be performed as fast as possible as carbonation of the freshly ground surface might otherwise occur.

The specimen is cleaned and allowed to dry before it is re-impregnated with fluorescent epoxy. This impregnation should also include the recently ground surface. It is recommended that excess epoxy be scraped off the ground surface while it is still soft leaving a layer approximately 1-2 mm thick, as this will facilitate the final polishing of this face.

The excess epoxy on the ground face is carefully removed after it has hardened by polishing on the diamond disc. Caution should be exercised during this grinding operation as the removal of too much material will leave too little impregnated concrete for the finishing operations. However, should this happen, one can recover the sample by re-impregnating the concrete and repeating the grinding of the face.

After cleaning and drying of the ground surface, a glass slide is mounted to the surface using an epoxy glue.

The specimen is now cut with a fine diamond saw parallel to the recently mounted slide approximately 1 mm from the slide. Once cut, the piece containing the auxiliary glass plate is saved/discarded.

The slide on the specimen is now mounted in a specimen holder on the lapping machine and ground down to a thickness of approximately 100 μm . The final polishing of the thin-section down to a thickness of 20 μm is performed by hand on the diamond disc. This part of the preparation requires great skill as the thin-section might otherwise end up being too thin, wedge shaped or feathered.

The polished face is covered with a cover glass by applying one drop of epoxy to the center of the concrete and carefully pressing the cover glass down vertically on the drop. It is important that no air bubbles are trapped underneath the cover glass as this would seriously reduce the quality of the thin-section.

Many of the above procedures resemble the procedures followed during the preparation of geological thin-sections. The major difficulties in preparing thin-sections from concrete are normally associated with tearing out the cement paste, especially around voids in the concrete and/or achieving an equal thickness over the entire thin-section. The latter problem can be especially difficult to avoid when thin-sections are prepared from concretes containing hard and dense aggregates.

Instrumentation

Evidently, the petrographic microscope plays a central role in the examination of the concrete thin-section. A detailed treatment of the construction and function of the

petrographic microscope can be found in other textbooks and will only be treated briefly in this report. The modifications of the standard petrographic microscope which are required in order to use the fluorescent light illumination technique are rather few and uncostly and will be treated during the description of the fluorescence technique.

Figure 1 is a schematic drawing of a "Leitz" petrographic microscope. The figure shows the most basic features and the light path in the instrument. The thin-section is placed on the rotating stage just below the objective. Light passes via a circular hole in the stage, up through the semi-transparent thin-section and further through the magnifying lens, the objective. Several objectives are mounted on a circular revolving nose which makes it possible to shift between several magnifications. It is thus possible to examine the thin-section in magnifications ranging from 25× to approximately 600×.

The light source needs to be more powerful than normally employed in petrographic microscopes if examination in fluorescent light is desired. It normally suffices to use a 100-W halogen lamp.

Examination of the thin-sections can be performed in four different modes:

- Ordinary light,
- Polarized light,
- Polarized light with compensator, and
- Fluorescence.

Ordinary light examination as illustrated in Figure 2a, is achieved by allowing the light from the light source to pass unhindered through the thin-section. Examination of the concrete in this mode makes all of the constituents of the concrete appear in their natural "transmitted light" color. Thus, quartz will appear white due to its lack of color, while fly-ash can show various shades from almost colorless to deep brown. The hardened cement paste normally has a buff colored appearance. Most minerals do, unfortunately, appear colorless in transmitted light in thin-section which often makes their distinction difficult. However, due to the crystalline characteristics of most minerals, it is possible to make further identifications by the use of polarizing light microscopy. Polarized light mode, shown in Figure 2b, is obtained by inserting a polarizing filter in the light ray before it passes through the thin-section. This filter, normally called the "polarizer" causes light from the lamp to oscillate in one direction, denoted "North-South" (N-S). Another polarizing filter, the "analyzer", is inserted in the light ray after it has passed through the thin-section only allowing light oscillating in the East-West (E-W) direction to pass through to the observer.

Thus, if light is allowed to pass uninterrupted from the polarizer to the analyzer, that is, if the thin-section is removed, the image seen in the eye pieces will be completely dark as all light passing through from the polarizer is absorbed by the analyzer.

However, the image will not be dark when the thin-section is inserted in the light path between the polarizer and the analyzer if birefringent material is present. When the light which has been forced to oscillate in one direction by the polarizer, passes through a

crystalline solid in the thin-section, such as quartz, or calcite in a limestone aggregate, the ray will be split into two oscillation directions. At the same time one of the rays will be delayed with respect to the other due to differences in refractive index. The actual mechanisms for this optical behavior of crystalline solids is rather complicated and the reader who wants further knowledge about these topics is referred to the crystal optical literature, for instance Phillips (1971). However, by treating the light emanating from the crystalline materials in the thin-section with the analyzer, a distinct coloration of birefringent minerals can be seen in the eyepiece. These colors assist the petrographer in distinguishing between the different crystalline solids in the thin-section. Materials which are either glassy, amorphous or belong to the cubic crystal system, do not alter the behavior of the polarized ray during passage. These materials will appear completely dark when viewed in polarized light; they are isotropic.

The difference between observation in polarized light and in polarized light with a compensator is that the compensator adds or subtracts a well known "retardation" to the rays emitted from the thin-section. This is seen in the microscope as a rather spectacular coloration of the polarized image, Figure 2c. This method is only used as an aid in the identification of minerals during examination in polarized light.

So far, only the examination devices available on the standard petrographic microscope, have been described. Application of the fluorescence method for the determination of w/c ratios and for the detection of flaws and inhomogeneities in the concrete requires a few additional accessories.

First, a monochromatic light source is required which is able to induce fluorescence in the epoxy in the thin-sections. The light should be monochromatic as excess light has to be filtered away after passage through the thin-section. The monochromatic illumination is obtained by inserting a filter designed to pass ultraviolet light (BG 12), in the light path before it enters the thin-section. This UV filter allows the passage of light with a wave length around 350 nm. Due to the large absorption of light during passage of the blue filter, it is necessary to use a powerful light source with an intensity around 100 W.

The fluorescent dye in the epoxy is excited by the UV light and emits yellow light with a peak intensity a little above 530 nm. By insertion of a yellow filter (K510 or K530) in the light path above the thin-section which absorbs all light with a wave length beyond 510 to 530 nm, the excessive UV light from the light source is filtered away. The resultant image in the eyepieces thus comprises the light emitted from the fluorescent epoxy only. As porous areas in the thin-section contain a higher portion of fluorescent epoxy, it follows that porous areas in the concrete thin-section appear bright while dense areas appear dark. This is shown in Figure 2d.

From the above principles it is evident that features such as microcracks, air voids, porous paste-aggregate interfaces etc. will appear bright yellow when viewed in fluorescent light. The coarse aggregates and the sand particles in the concrete are normally so dense that they appear dark green in fluorescence. An aggregate with zero porosity should theoretically be completely dark, but in practice it may appear dark green.

The hardened cement paste, however, displays varying "brightness" depending on the amount of epoxy impregnated capillary voids in the cement paste.

As shown in Figure 3 the amount of capillary voids is closely related to the amount of water used in the mix, i.e. the water-cement (w/c) ratio. The figure shows that assuming that the water is capable of completely hydrating all the cement present, the only capillary voids left in the cement paste will be those caused by the chemical shrinkage of the cement - that is the volume reduction associated with the reaction: cement + water \rightarrow hydrated paste. Complete hydration theoretically occurs at a water/cement ratio of 0.40. Increasing the w/c ratio leads to the presence of an increasing surplus water which is located between the hydration products in small capillary voids, i.e. as capillary water.

Decreasing the w/c ratio below 0.40 leads to the presence of unhydrated relics of cement grains as the amount of water was insufficient to cause complete hydration of the cement.

However, the assumption of complete hydration of the cement rarely holds true in real concrete structures. Investigation of old concrete structures shows that between 20 and 25% of the cement grains still remain unhydrated after several years. Consequently, it is still possible to observe capillary pores in concretes with a w/c ratio below 0.30.

These observations suggest that a cement paste with a low w/c ratio would absorb less epoxy than a cement paste with a higher w/c ratio. If the thin-sections of two such cement pastes are compared in fluorescent illumination, it follows that the paste with the low w/c ratio would appear darker than the paste with the high w/c ratio. Figures 4a and b which show the appearance of mortars with w/c ratios of 0.40 and 0.60, respectively, confirms this theory. By preparing thin-sections from mortar bars with known w/c ratios, a series of standards can be obtained which vary in brightness as a function of w/c ratio. These standards can then be used to determine the w/c ratio of a sample of an unknown concrete mix. Skilled operators which use these methods are capable of determining the w/c ratio of an unknown concrete specimen with an accuracy of better than 0.1 often 0.03 (see following report data). However, less skilled operators will have a harder time, but with practice and proper standards should be able to determine the w/c ratio of hardened cement paste to ± 0.1 or better.

Examination of Fluorescent Thin-Sections

The determination of the w/c ratio of an unknown concrete specimen should not be carried out before the thin-section has been examined thoroughly in ordinary and polarized light. There are several reasons for this warning. First, it is extremely important to check the thin-section for flaws induced during the preparation which could affect the w/c determinations. Second, one must ensure that the cement paste is suitable for w/c determination with regards to both composition and potential secondary alteration of the paste, e.g. carbonation.

Due to the large differences in hardness between the aggregates themselves and between the aggregate and the cement paste, it is often difficult to achieve an equal thickness of 20 μm

over the entire face of the thin-section. The determination of the w/c ratio depends on having an equal thickness of the thin-section. A reduction in thickness leads to a reduction in the total amount of fluorescent epoxy and consequently a darker fluorescent image. Figures 5a and b are micrographs of two concrete mixes with the same w/c, recorded in fluorescent light. The thin-section in Figure 5b is only 10 microns thinner (but 50% thinner) than the thin-section in Figure 5a. The apparent reduction in brightness when going from a to b is seen to be quite significant. Hence, if the thin-section is too thick, this would result in an apparent w/c ratio higher than the actual value and vice versa. It is therefore important to check the thickness of the thin-section by observing the interference colors of the minerals in the sand and in the coarse aggregates. The interference color of quartz is a good indicator as this mineral is almost always present in the aggregates. The interference color of quartz should be a first order white or grey ($\sim 20\ \mu\text{m}$ thick). A yellow color signifies too great a thickness ($\sim 30\ \mu\text{m}$ thick) while dark grey signifies a too small thickness ($\sim 10\ \mu\text{m}$ thick) of the thin-section.

Another problem which is often encountered in fluorescent thin-section analyses is caused by insufficient impregnation. This can either be due to the presence of a very dense paste or poor impregnation procedure. One should therefore check especially the small voids in the thin-section in ordinary light to see whether these are completely filled with the yellow epoxy.

It is also a good idea to check the color and homogeneity of the impregnating epoxy in larger voids in the thin-section. If the epoxy appears too pale or too yellow this could indicate a wrong dosage of dye during the preparation of the fluorescent epoxy. Likewise, inhomogeneities in the color distribution could indicate insufficient mixing of the epoxy.

Several other undesirable phenomena caused by the preparation procedure could be mentioned but the items mentioned above appear to be the most common, and most significant in their effect on the w/c determination.

Assuming the thin-section is adequate, one proceeds to the examination of the hardened cement paste itself in order to verify whether it is suitable for w/c determination. This task is especially important if the composition of the cement is unknown, as blended cements or cements intermixed with a filler can yield misleading apparent w/c ratios when examined by the fluorescence method.

Blended cements are cements intermixed with a mineral admixture such as silica fume, fly-ash or slag. If the silica fume has been added to the concrete as a slurry it is often difficult to determine its presence by thin-section microscopy.

The reason for this is that the silica fume particles are very small ($\sim 0.01\ \mu\text{m}$). Close examination of the hardened cement paste under high magnification (500-600 \times) in ordinary light can, however, sometimes reveal the presence of small agglomerates of silica fume. See Figure 6. It is also possible to get an indirect indication of the presence of silica fume in an unknown concrete mix as the cement paste tends to be significantly darker than normal, when viewed in polarized light. The reason for this is that a large part of the disseminated calcium hydroxide in the hydrated paste has reacted with the silica fume.

Slag and fly-ash are easily discernible in thin-section. Slag occurs as angular, glassy fragments with approximately the same size as the cement grains. See Figure 7. The slag particles will appear completely dark in polarized light as they consist primarily of isotropic glass.

Fly-ash is seen in the hydrated paste as massive and hollow spheres with colors varying from colorless to yellow, brown and black.

The presence of a filler in the cement is normally quite easily recognized as the filler is almost always calcium carbonate (CaCO_3). The presence of such a filler provides the cement paste with a brighter appearance than normal, when viewed in polarized light. The same appearance of the cement paste can occur, however, if the polished surface of the concrete was allowed to carbonate during preparation of the thin-section.

Carbonation due to the weathering of concrete structures is seen in polarized light as an irregular, amber colored front which extends from the exposed surface and into the sample.

It is important to avoid carbonated cement paste when the w/c determinations are performed as carbonated paste in some cases can be denser than the original paste and in some instances, more porous.

Having checked the quality of the thin-section and the composition of the hardened cement paste, the determination of the water - cement ratio can now proceed.

The microscope is equipped with a combination of objectives and oculars so that the total magnification is somewhere around 65x. The UV filter (BG 12) and the yellow filter (K510 or K30) are inserted into the light path and the intensity of the light is increased to approximately 100 W. To ensure a sufficient intensity of light, it is recommended that the iris diaphragm be open and that the polarizer be removed from the light path.

Having focussed the image, one randomly selects 10 areas in the thin-section and evaluates in each case the w/c ratio of the paste. By selecting 10 sites in the thin-section the effects of inhomogeneous mixing and dispersion of the cement paste is avoided. The average of the 10 measurements is considered to be the w/c ratio of the concrete in question. It is advisable to perform the measurements a few mm away from the edges of the thin-section as light flare from the surrounding rim of epoxy, may increase the brightness of the paste and hence the apparent w/c ratio.

By thoroughly practicing the technique, accurate w/c determinations can be carried out without constant references to the standards. It is, however, recommended that reference to the standards be made from time to time. Experience shows that the petrographer normally does not have difficulty in distinguishing w/c ratios in steps of 0.02-0.03, but it is often observed that the measured values generally tend to become too high or too low if regular checks of the standards are not made.

References

- W.U. Ahmed, Improvements in Sample Preparation Technique For Microscopic Analyses of Clinker and related materials" Proceedings of The 5 International Conference on Cement Microscopy, Nashville Tennessee, USA, 1983.
- K.T. Andersen and N. Thaulow, "The study of Alkali-Silica reactions in Concrete by The Use of Fluorescent Thin-Sections" Symposium on Petrography Applied to Concrete, ASTM, St. Louis, June 1989.
- A. Damgaard Jensen, "Investigation of Concrete by Analyses of Thin-sections" IABSE Symposium on Strengthening of Building Structures, Venice, 1983.
- A. Damgaard Jensen, "Strukturanalyse af Beton" (Structural Analyses of Concrete), Beton Teknik, Cto, Denmark, 1985. (in Danish)
- H. Gudmundsson, S. Chatterji, A. Damgaard Jensen, N. Thaulow and P. Christensen, "Quantitative Microscopy as a Tool For The Quality Control of Concrete" Proceedings of The 3 International Conference on Cement Microscopy, Nashville Tennessee, USA, 1981.
- B. Mayfield (1990), "The Quantitative Evaluation of the Water/Cement Ratio Using Fluorescence Microscopy," Magazine Concrete Research, 42, 45-49 (1990).
- Nordtest 677-87, "Concrete, Hardened: Water-Cement Ratio," Nr. 677-87.
- W.R. Phillips W. R., "Mineral Optics - Principles and Techniques," Freeman, 1971.
- E. Soers, "Preliminary Results on a Petrographical Examination of Alkali-Silica Reactions in Belgium" Proceedings of The 10 International Conference on Cement Microscopy, San Antonio, Texas, USA, 1988.
- N. Thaulow, A. Damgaard Jensen, S. Chatterji, P. Christensen and H. Gudmundsson, "Estimation of The Compressive Strength of Concrete Samples by Means of Fluorescence Microscopy" Nordisk Betong, No 2,4, 1982.
- N. Thaulow, K.T. Andersen and J. Holm, "Petrographic Examination and Chemical Analyses of The Lucinda Jetty Prestressed Concrete Roadway", 8 International Conference on Alkali-Aggregate Reaction, Kyoto, Japan, 1989.
- H.N. Walker and B.F. Marshall, "Methods and Equipment Used in Preparing and Examining Fluorescent Ultrathin Sections of Portland Cement Concrete," Cement, Concrete and Aggregates, CCAGDP 1 (1), 3-9, 1979.
- H.N. Walker, "Evaluation and Adaptation of the Dubrulov and Romer Method of Microscopic Examination of Hardened Concrete," VA Highway and Transportation Research Council, Charlottesville, VA, April 1979, VHTRC 79-R42 (60 pp).

W. Wilk, G. Dubrolubov and B. Romer, "Development in Quality Control of Concrete", TRR 504, Transportation Research Board, 1974.

W. Wilk and G. Dubrolubov, "Microscopic Quality Control of Concrete During Construction" Proceedings of the 6th International Conference on cement Microscopy, New Mexico, 1984.

3

Examination of SHRP 1-19 Concrete Samples

Introduction

The present examination of 19 concrete samples was carried out as part of the activities under the SHRP-C-201 project, "Concrete Microstructure" which deals with the microstructural characterization of hardened cement paste in concrete.

The objective of this examination was to assess and possibly quantify the porosity variations occurring in the hardened cement paste. These porosity variations were determined by the use of fluorescence microscopy of concrete thin sections as described in Part One of this report. By stimulating a yellow fluorescence from a dye-impregnated region by a deep blue UV light through a thin section, porous areas will appear bright yellow-green while the dense areas will appear dark green.

Samples

Nineteen concrete samples were received and identified as follows:

MRL No.	GMIC No.	T.S. No.	Received
S89-1Ma	389-1	3113-1	24 April 89
S89-2Ma	389-2	3113-2	24 April 89
S89-3M28a	389-3	3114-1	24 April 89
S89-4M28a	389-4	3114.2	24 April 89
S89-5Mb	689-1	3171-1	29 May 89
S89-6Mb	689-2	3171-2	29 May 89
S89-7Mb	689-3	3171-3	29 May 89
S89-8	409-1	3278-2	27 June 89
S89-9	409-2	3278-1	27 June 89
S89-10	889-1	3171-4	27 July 89
S89-11	1289-1	3196-1	11 Sept. 89
S89-12	1289-3	3196-4	11 Sept. 89
S89-13	1289-2	3196-3	11 Sept. 89
S89-14	1689-1	3261-1	2 Oct. 89
S89-15	1689-3	3261-3	2 Oct. 89

S89-16	1689-2	3261-2	2 Oct. 89
S89-17	0690-1	3284-1	5 Feb. 90
S89-18	0690-2	3284-2	5 Feb. 90
S89-19	0690-3	3284-3	5 Feb. 90

One thin section was prepared from each sample.

The heading "T.S." refers to the number assigned to the thin section prepared from the concrete samples. Specifics regarding the mix design, water-cement ratio, etc., for the concrete samples are presented, together with the quantified results from the microscopic examination and illustrative micrographs in a series of tables and figures. The data regarding mix designs were obtained from the Second Quarterly Report, Year Two, presented to SHRP July 17, 1989 and the Third Quarterly Report, Year Two, presented to SHRP October 17, 1989.

Specifics regarding the mix design, w/c ratio, etc., for the concrete samples are presented in the following pages together with the quantified results from the microscopic examination.

Microstructural Data

As the work proceeded, so did the quantitative nature of the results. The microstructural features found in SHRP 89-1 to 7 thin sections were evaluated using a numerical scale ranging from 0 to 3. The following (qualitative) terms are used to describe the individual grades:

- 0: Not present, insignificant.
- 1: A little, of minor importance.
- 2: Clearly present, significant.
- 3: Dominant, severe.

In addition, due to the potential significance of porous zones around the coarse aggregates (Figures 9, 11, 12 and 14) and their effect on permeability, an attempt was made to determine the fractional percentage of porous zones around these aggregates. An average value was obtained by estimating the percentage of porous zones at the interface of the individual coarse aggregates in the entire thin section.

Two other parameters were determined in order to quantify the microstructure:

- (1) The surface area of the coarse aggregates per unit volume of concrete (cm^2/cm^3) was determined by combining line intercept and point counting data for the coarse aggregates in cross sections of the concrete cores, and
- (2) The intersection per unit length of test line with the microcracks in the thin sections.

From the microcrack line intercept, the average line intercept in cm and the surface of the crack planes per unit volume can be estimated. Similarly the specific surface of the coarse

aggregates and the mean free distance between them can be determined (see Underwood, 1970).

As work progressed, the use of quantitative stereology was emphasized and in the cases where microstructural features are now described by stereological methods, earlier semi-quantitative terms (S89-1 to 7) have been omitted. The following section explains the measurement and meaning of the stereological parameters presented during the microscopic examination of samples S89-1 to 19 (summarized in Table 1).

Stereological Measurements

Measurements have been performed on cut slices of concrete and on thin sections. Point counting and the linear traverse method have been used on the cut slices to obtain information about the amount and surface area of the coarse aggregates. Fluorescent thin section studies combined with linear traverse method have provided information about the amount of microcracking in the concrete.

Referring to Table 1, features listed under the heading "MICROSCOPY" have been measured using stereological methods. A short description of each of these features is presented below:

V_v, Volume, coarse aggregate: The volume of coarse aggregate is determined by simple point counting on the cut slices of concrete. This value is used in the calculation of lambda which is defined later in the text.

P₁, line intercept coarse aggregates: Represents the number of paste/aggregate intercepts per unit length of testing line. Also see ASTM C457. Several lines are drawn on the cut concrete slices and the number of intercepts with paste/aggregate boundaries are registered. This number is divided with the total line length and the result is presented as P₁.

S_v, surface of coarse aggregates per test volume: According to the rules of stereology, the surface to volume ratio, S_v, can be calculated as 2P₁. The surface to volume ratio expresses the surface area of the coarse aggregates per unit volume of concrete. This value will increase with a decreasing aggregate size and an increasing amount of aggregates.

Lambda, mean free distance between coarse aggregates: This value expresses the average distance between the coarse aggregates and is calculated as

$$\frac{2x(1 - V_v)}{P_1}$$

P₁, line intercept cracks: This value is measured in the thin section in fluorescent illumination and expresses the number of intercepts of microcracks per unit length test line. It is here important to realize that although cracks are seen as lines in the thin section, they are in fact planar structures.

L, mean free distance between cracks: Expresses the average distance between cracks per unit volume of mortar; that is, exclusive of coarse aggregates. The value is calculated as:

$$\frac{(1-V_v \text{ aggregates})}{P_l}$$

The value is normalized per volume mortar as this operation makes the L values from different concrete mixes straightforward comparable.

Epsilon, cracks: This value represents the fraction of the paste/aggregate interface which appears porous or cracked when viewed in thin section in fluorescent light. This value has been established by measuring the length of the periphery of the individual coarse aggregate particles in thin section and subsequently by measuring the length of the porous or cracked paste/aggregate interface.

General Examination

Samples S89: 1Ma, 2Ma, 3M28a and 4M28a

These four concrete samples are treated together as they represent concrete mixes with similar cement-aggregate ratios, slumps and w/c ratios. See Tables 1-5 and Figures 8-11. Figure 8(a) shows sample S89-1Ma in normal transmitted light, while 8(b) shows the same concrete in reflected fluorescent light. The other figures are all thin sections in transmitted light.

The four concrete samples have a coarse aggregate content consisting of a crushed limestone while the sand primarily consists of single- and polycrystalline fragments of quartz.

A narrow zone of cement paste with a high porosity and/or cracks is occasionally seen at the interface between the coarse aggregate particles and the surrounding hardened cement paste. The same zone is seen around a few schistose aggregates. Furthermore these particles also exhibit signs of internal cracking which is probably due to drying shrinkage of the particles.

The cement paste is homogeneous both in macro- and micro-scale.

The concrete contains some microcracks which are seen to interconnect several of the sand particles in the cement paste. It is not clear why these cracks have formed.

Samples S89: 5Mb, 6Mb and 7Mb

The compositional difference between these three concrete mixes and the four mixes mentioned above is that these samples contain a higher amount of aggregate and have been made with the addition of a superplasticizer. The specific mix compositions are presented in Tables 6-8 and data are presented in Tables 1, 6-8 and Figures 12-14.

Examination of the hardened cement paste in fluorescent light shows that sample No. 5Mb in particular possesses a rather inhomogeneous microstructure. Also, the w/c ratio for this sample was measured as 0.42 although the accompanying mix specifications states a w/c of 0.47. Concrete S89-6Mb in transmitted fluorescent light (Fig. 13a) as well as in reflected fluorescent light (Fig. 13b) both show a homogeneous microstructure.

Samples S89: 8 and 9 (Tables 1, 9, 10, Figures 15, 16)

These two samples represent concrete mixes with differing water-cement ratios, 0.42 and 0.53, respectively. It should be noted that a superplasticizer has been added to sample S89-8 (Figure 15). These two concrete samples are generally quite homogeneous as viewed in thin section (Figures 15, 16) but it is noted that sample S89-9 (see Figure 16) contains significantly fewer microcracks and porous paste/aggregate interfaces than the rest of the concrete samples examined, despite its higher w/c ratio.

Samples S89: 10, 11, 12 and 13 (Tables 1, 11-14, Figures 17-20)

These concrete samples are treated together as they represent concretes with a fixed binder to aggregate ratio and a fixed aggregate size. The difference between the concrete samples is comprised by the substitution of a part of the cement with slag, two types of fly ash and silica fume, respectively.

Sample S89-10 has, according to the mix formulation, a slag content of 40% by weight of binder. The slag particles are clearly seen in thin-section as small, transparent glass shards in the hardened cement paste. See Figure 17a. They are also easily distinguishable in polarized light as their glassy nature causes them to appear completely dark.

The porosity of the paste is very low when viewed in fluorescent light. As Figure 17b shows, most of the paste appears very dark which indicates an "equivalent" water-cement ratio below 0.35. These observations tend to be in conflict with the calculated water-(cement+slag) ratio which is reportedly 0.47.

Figure 17 also shows that the amount of microcracking in the paste is quite significant. Likewise, porous paste/aggregate interfaces appear to be quite common in this thin-section.

Sample S89-11 comprises a concrete mix with a substitution of 20% by weight of the cement with a Class F fly ash. As shown in Figure 18a this fly ash often contains rather large hollow spheres of glass. The amount of microstructural inhomogeneities is rather low in this concrete mix. The fluorescence images (Figure 18b) show that the dispersion of the cement and fly ash is good and that the number of microcracks and paste/aggregate porosities is rather low.

Sample S89-12 represents another concrete mix with fly ash addition. The percentage of cement replaced by fly ash is the same as for Sample S 89-11 but the fly ash is a Class C fly ash. This type of fly ash is seen in thin-section to be smaller in average grain size than

the Class F fly ash, previously examined. Likewise, a larger portion of this fly ash is constituted by massive spheres of glass as seen in Figure 19a. Under fluorescent light, the microstructure of this concrete mix resembles the microstructure of Sample S 89-11, that is, a rather homogeneous dispersion of the binder and a low amount of microcracks and paste/aggregate porosities, see Figure 19b.

Sample S89-13 has been prepared with silica fume constituting 7.5% by weight of the binder material (silica fume+cement). During examination of concrete with silica fume added, it is normally observed that the cement paste achieves a hazy appearance when examined in thin-section in polarized light. Likewise, the hardened cement paste normally appears dark due to the removal of the disseminated calcium hydroxide in the paste. In fact, in this way the slag and silica fume pastes bear a greater resemblance to each other than to the other materials. A certain lack of $\text{Ca}(\text{OH})_2$ in the paste is observed in the thin-section prepared from Sample S89-13. See Figure 20a. However, as the paste did not appear particularly hazy and as it was not possible to detect any agglomerations of silica fume in the paste, even at high magnifications, it was not possible to obtain a positive identification of silica fume by the thin-section technique. The fluorescent examination revealed a fair amount of micro cracks in the paste and porosities at the paste aggregate interface. See Figure 20b.

Samples S89: 14, 15 & 16 (Tables 15-17, Figures 21-23)

These samples represent concrete mixes where the normal coarse, #67 limestone aggregate has been substituted with #8 limestone aggregate, #67 siliceous gravel and #8 siliceous gravel, respectively.

The differences between the microstructure of the hardened cement paste in the three samples are generally very small (Figures 21-23). They all exhibit a minor amount of microcracking and porosities at the paste-aggregate interface and the light variations in the dispersion of the cementitious particles in the paste do in all three incidents classify them as "grade 1" in terms of micro-inhomogeneity.

Hence, it does not appear that the reduction of the aggregate size and/or the change to siliceous gravel has any noticeable effect on the microstructure of the concrete samples.

Samples S 89: 17, 18 & 19 (Tables 1, 15-17, Figures 24-26)

Although the exact mix compositions were not present at the time of preparation of this report, it clearly appears from the stereological measurements (Figures 24a, 25a, 26a) that these three concrete samples have a decreasing content of quartzite coarse aggregate in the order S89-17, 18 to 19. It also appears that the decrease in the coarse aggregate content has been counteracted by an increase in the content of fine aggregate.

The fluorescence studies (Figures 24b, 25b, 26b) show that the samples have been prepared with different water-cement ratios as sample S89-17 has a w/c of 0.40-0.45, 18 has a w/c around 0.35 and 19 has a w/c of approximately 0.35-0.40.

The frequency of microcracking and porous zones along the paste/aggregate interfaces appear within the normal range when compared to the samples earlier examined.

Alternate Methods

As an alternate, one can examine polished sections rather than thin sections. Figure 27 illustrates differences in surface relief resulting from a decreasing w/c ratio. The upper sample is SHRP S89-9 (w/c = 0.53), and the lower sample is SHRP S89-8 (w/c = 0.42). Other than this difference, formulations are identical. Photos are ~50 \times . Much more relief in S89-9 is present, as a result of polishing. This is probably due to lower matrix strength of S89-9 compared to S89-8, the paste has been eroded. Upper photo also suggests more cracking and more porosity at interfaces. The crack in the lower figure is most probably an artifact caused by cutting of the sample.

Figure 28 demonstrates the effects of packing on density. The upper sample is SHRP S89-5 (w/c = 0.47) and the lower is SHRP S89-4 (w/c = 0.47). S89-4 has a higher cement content (8 bags/cubic yard) than S89-5 (6.25 bags/cubic yard).

In addition S89-5 has a lower sand/aggregate ratio than S89-4. Even though S89-5 has higher strength than S89-4, S89-5 still appears rougher. The matrix is not as strong and polishing relief is higher. Particles from the paste have been plucked during polishing. The increased strength is apparently the result of improved packing (S89-5) not the matrix strength itself (S89-4).

References

E.E. Underwood, Quantitative Stereology, Addison-Wesley Publishing Company, Reading, MA (1970), 274 pp.

4

Discussion

The investigation of concrete in thin section is a powerful tool both for development and forensic applications. But, because it is a "learned" technique, at present it cannot be fully implemented by an unskilled operator.

Standards are necessary and difficult to make. Thin sections must always be exactly the same thickness over the entire section and from sample to sample. The preparation and polishing is an art in itself. Great care must be exercised to prevent the inadvertent introduction of microcracks (see for example, Struble's papers NBS IR 88-3702 and NBS 87-3504).

However, once these hurdles are overcome, the technique can be very useful. It can be used to evaluate homogeneity of mixing, dispersion of aggregates, effectiveness of superplasticizers, etc. The ability to better observe alkali silicates, carbonation, sulfate attack, microcracking, etc., is self evident. Our recommendation is to implement the technique, but develop automated computer-assisted data interpretation as much as possible.

Preliminary observations were made on some of the fluorescent epoxy impregnated specimens in reflected light. Although some features show up well, the amount of information does not appear to be equal to that in the thin sections. However, the concurrent examination of the polished sections can provide some important information on relative matrix strength related to variations in w/c and packing.

References

- L. Struble and E. Byrd, "Epoxy Impregnation of Hardened Cement Pastes for Characterization of Microstructure," NBSIR 87-3504 (1986).
- L. Struble and P. Stutzman, "Epoxy Impregnation Procedure for Hardened Cement Samples," NBSIR 88-3702 (1988).

Appendix A

Figures

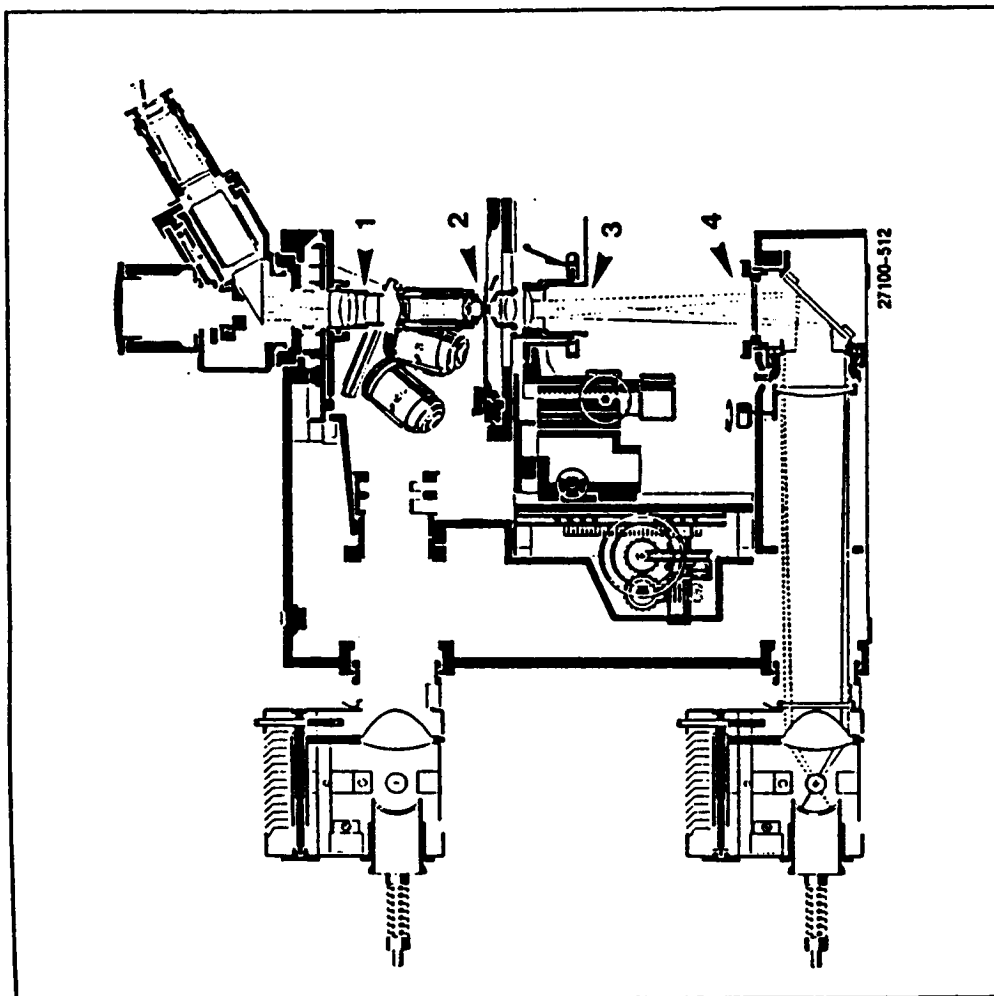


Figure 1. Schematic drawing of a "Leitz" petrographic microscope. Pathway of light and the location of the thin-section and auxiliary filters are shown.

- 1: Slot for compensator or yellow filter
- 2: Location of thin-section
- 3: Location of polarizing filter
- 4: Location of blue filter, BG-12

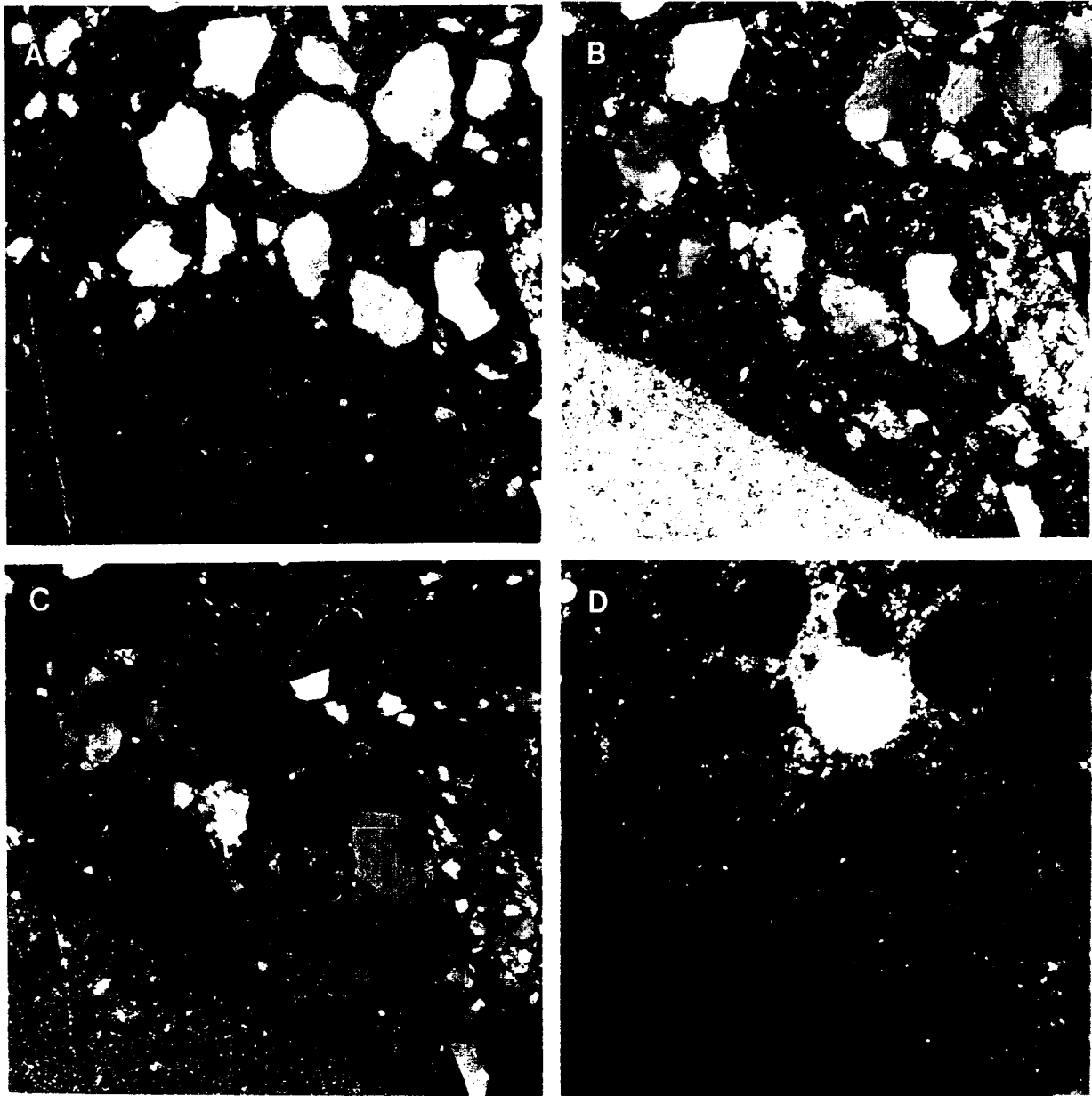


Figure 2. Micrograph of concrete recorded in: (a) Ordinary light, (b) Polarized light, (c) Polarized light with compensator and (d) Fluorescence. Field of view: 2.5×2.5 mm.

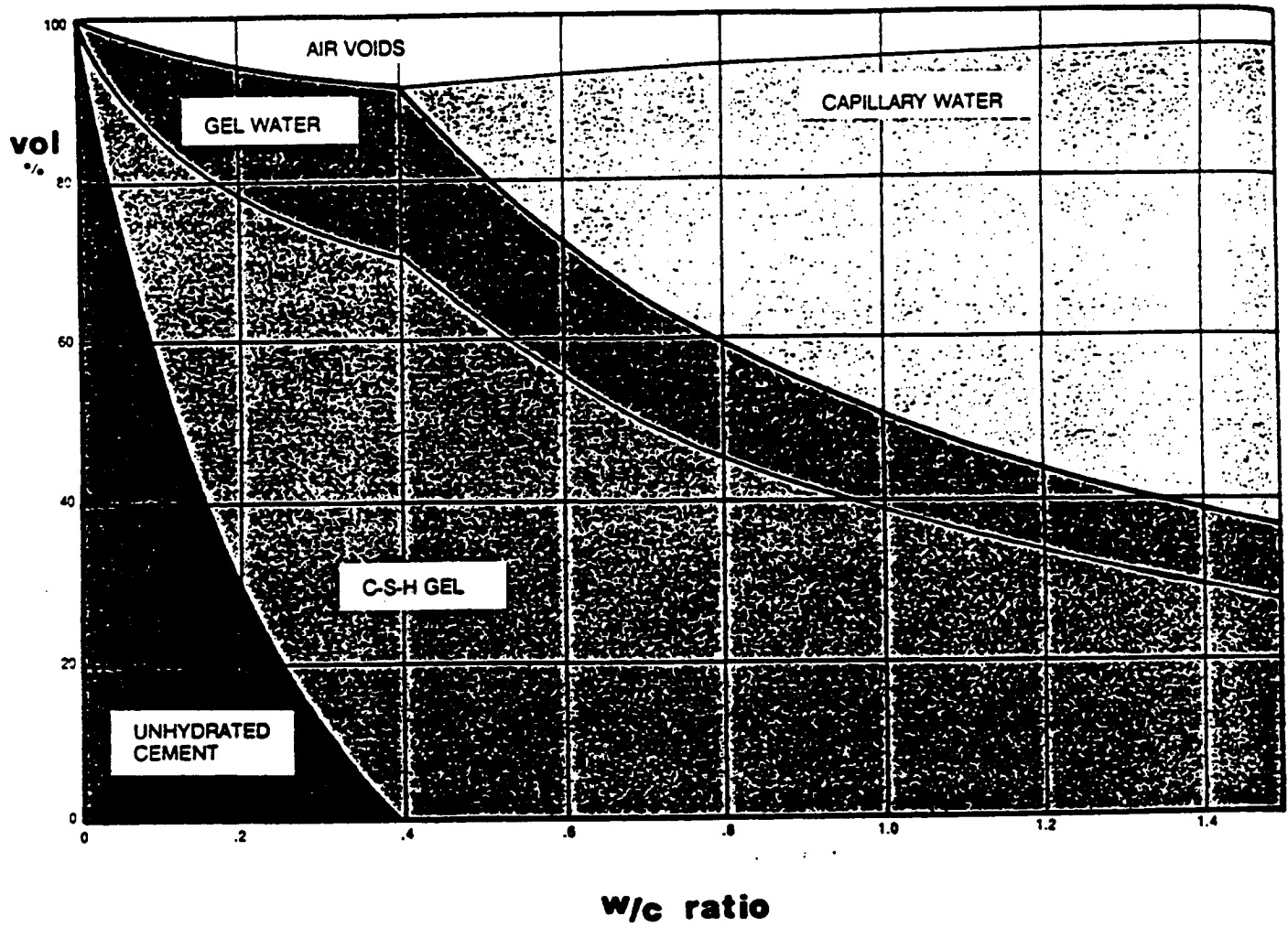


Figure 3. Diagram depicting the distribution of unhydrated cement, C-S-H gel, gel water, capillary water and chemical shrinkage voids as a function of the w/c ratio.

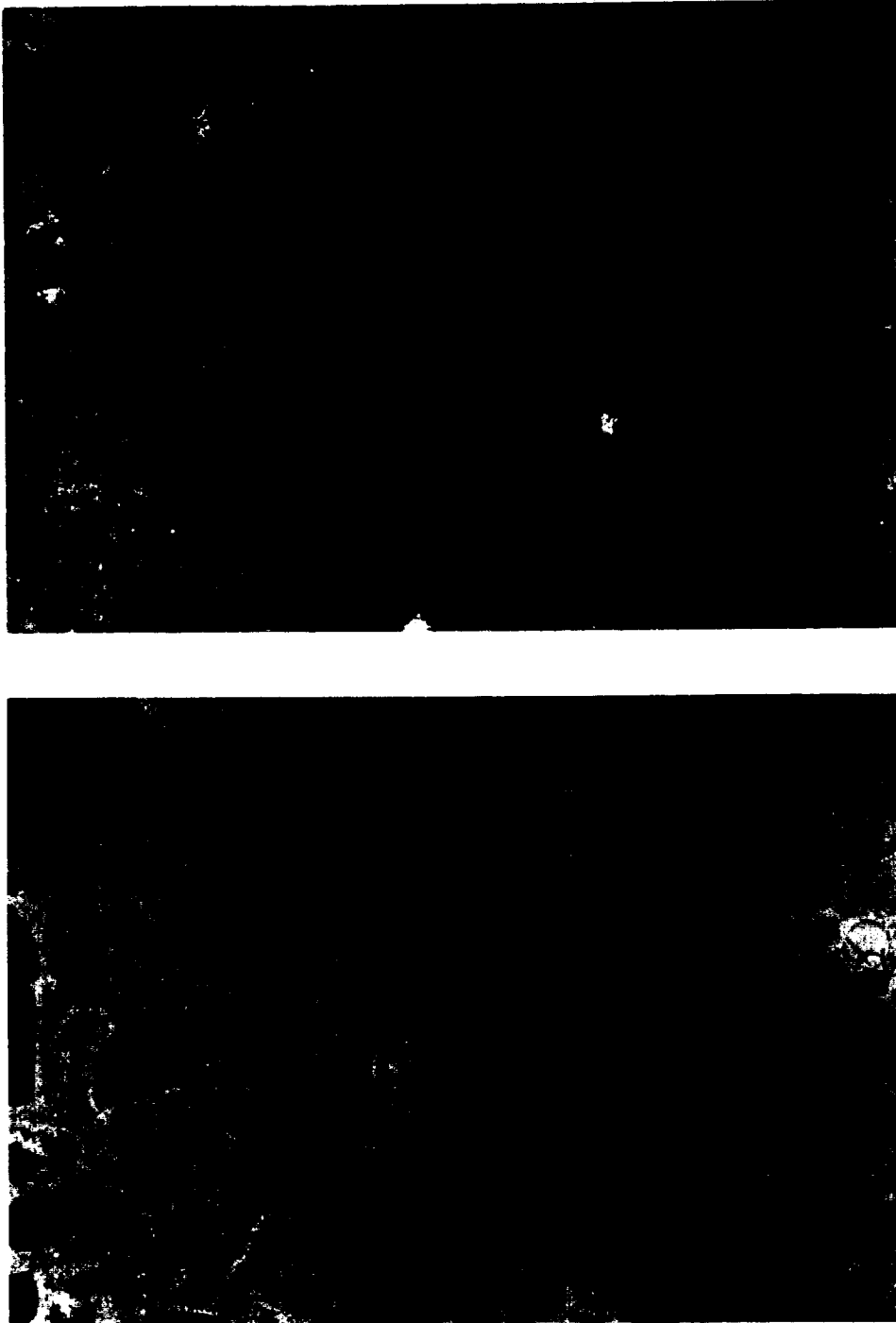


Figure 4. Micrographs of thin-sections prepared from mortars with a w/c ratio of 0.40 (top) and 0.60 (bottom), respectively. The images show that the paste with a w/c of 0.40 appears significantly darker in fluorescence than the paste with w/c 0.60. Field of view: 3.9×2.7 mm.

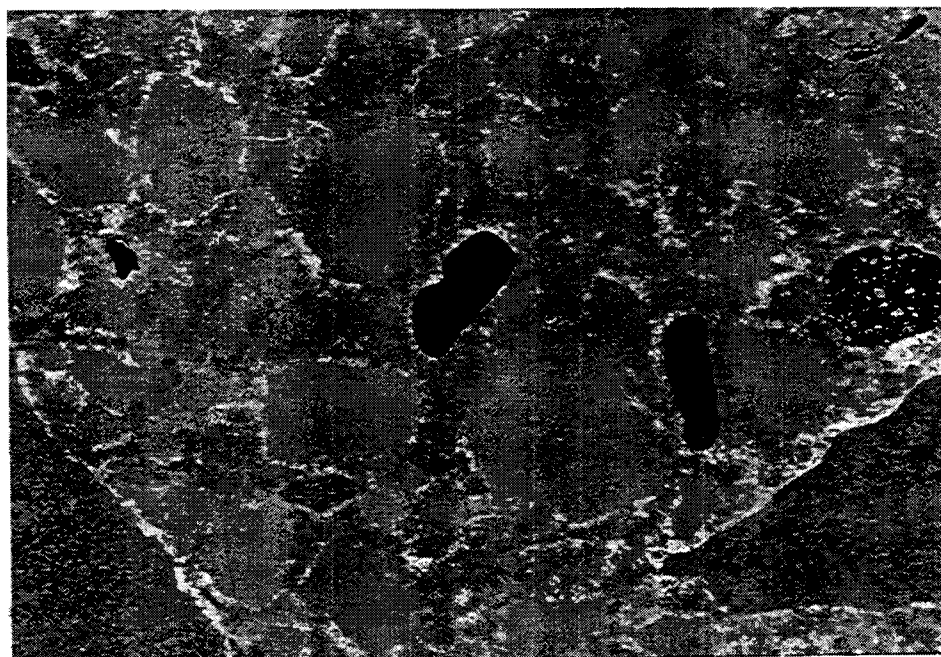
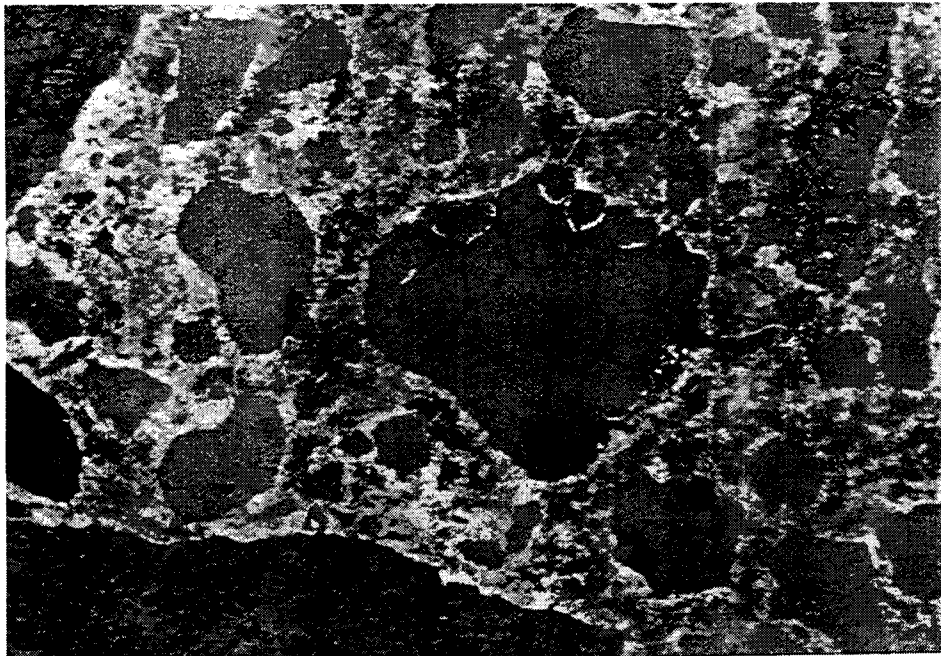


Figure 5. Fluorescent images of two thin-sections with similar w/c ratio but 10 μm difference in thickness. Note the apparent change in w/c ratio on going from 20 μm (top) to 10 μm (bottom). Field of view $1 \times 1.5 \text{ mm}$.



Figure 6. Micrograph of the hardened cement paste of a concrete intermixed with approximately 7% silica fume. The presence of silica fume is revealed by the presence of small globules of agglomerated silica particles . Ordinary light. Field of view 0.12×0.16 mm.

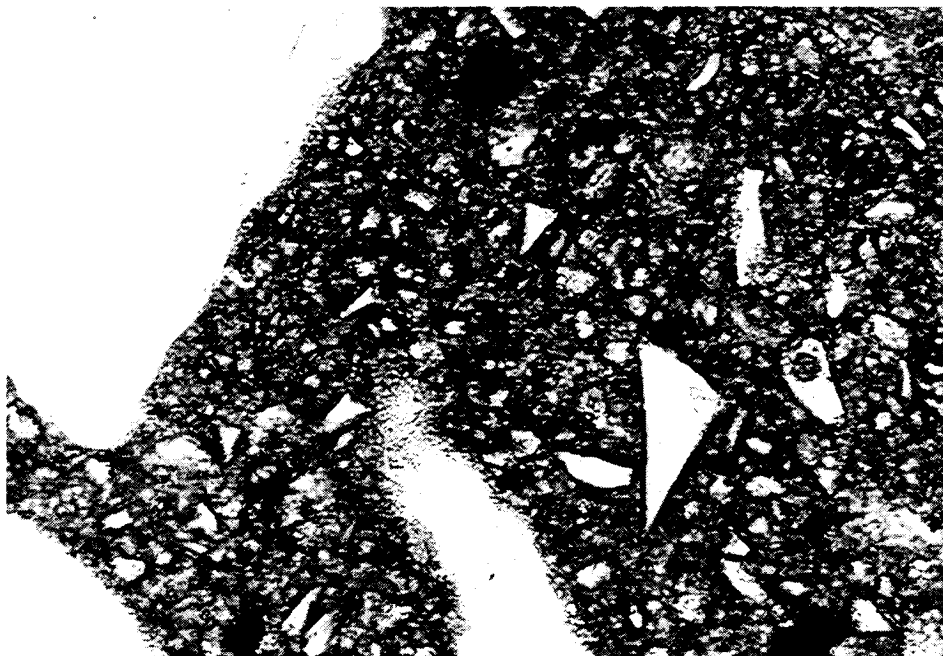
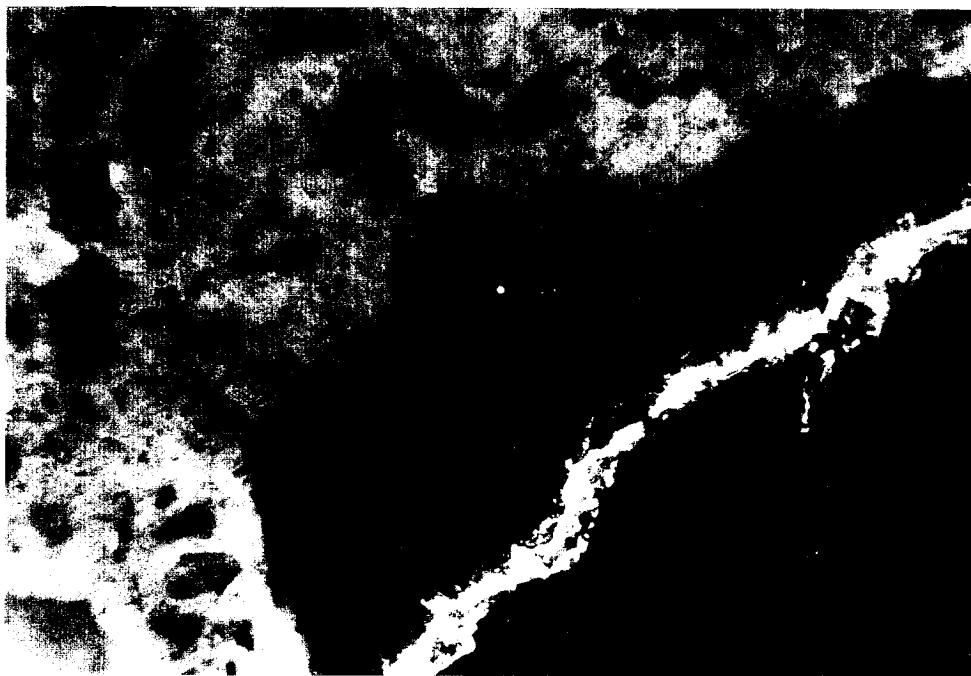


Figure 7. Micrograph of slag cement. The slag particles are easily discerned as small angular shards of transparent glass. Ordinary light. Field of view: 0.27×0.16 mm.

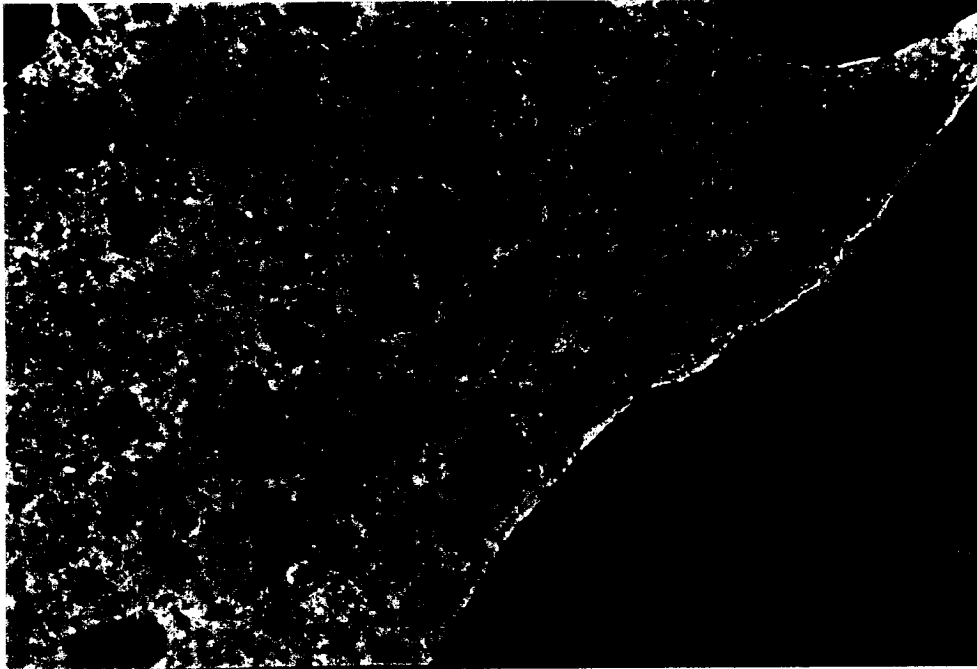


(a)

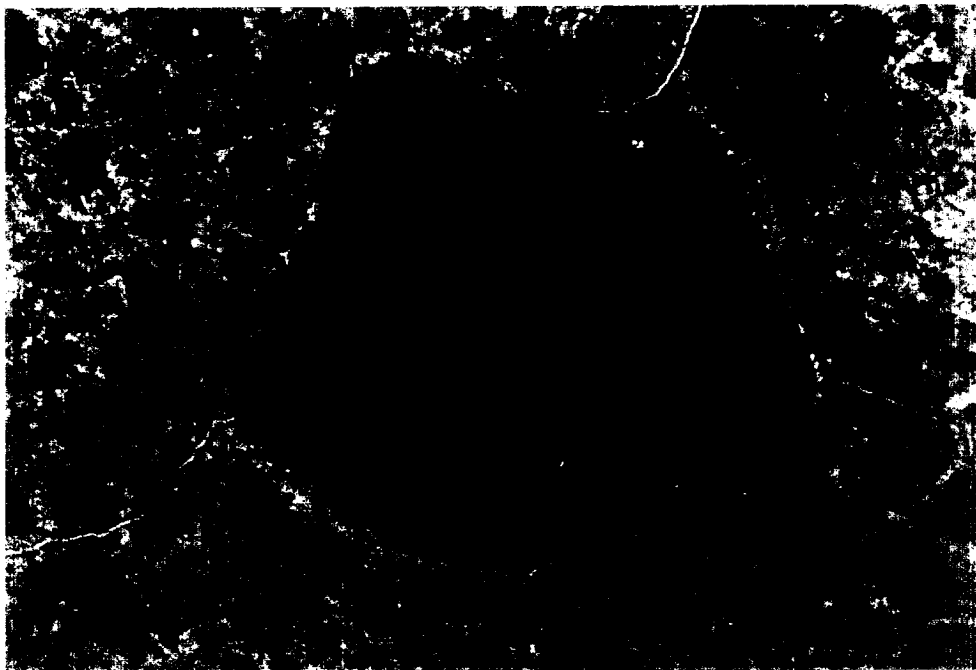


(b)

Figure 8. Micrographs of sample S89-1Ma. Fluorescence 2.7×3.9 mm. (a) The thin section shows the appearance of the hardened cement paste in fluorescent light. The paste is homogeneous with a water-cement ratio of 0.46. (b) Image of same specimen in reflected fluorescent light. Note transluence of sand grains, and the sharp contrast in the crack in the aggregate.

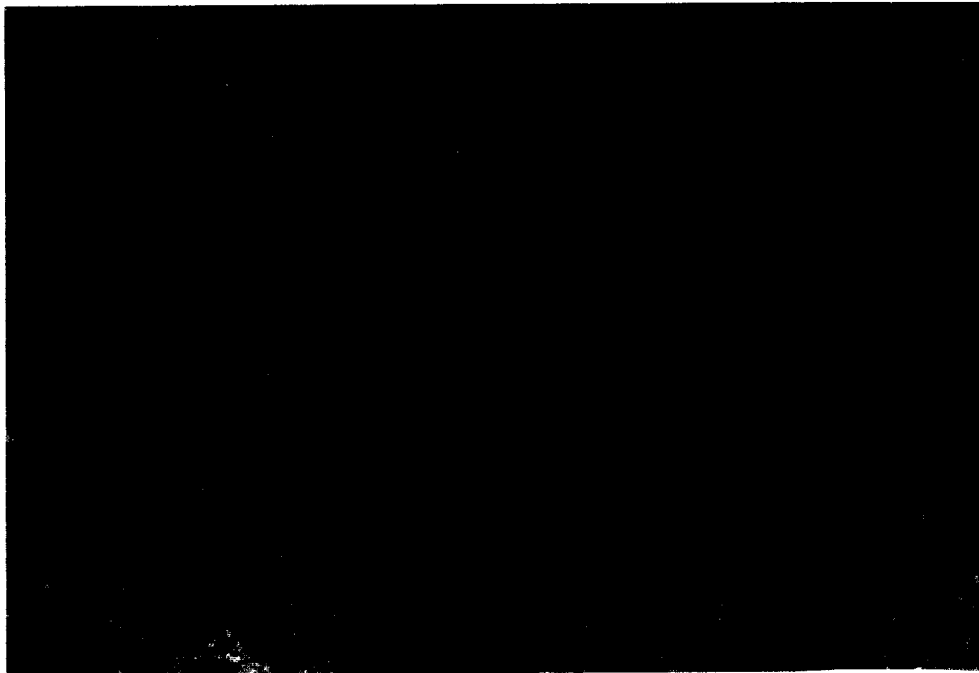


(a)

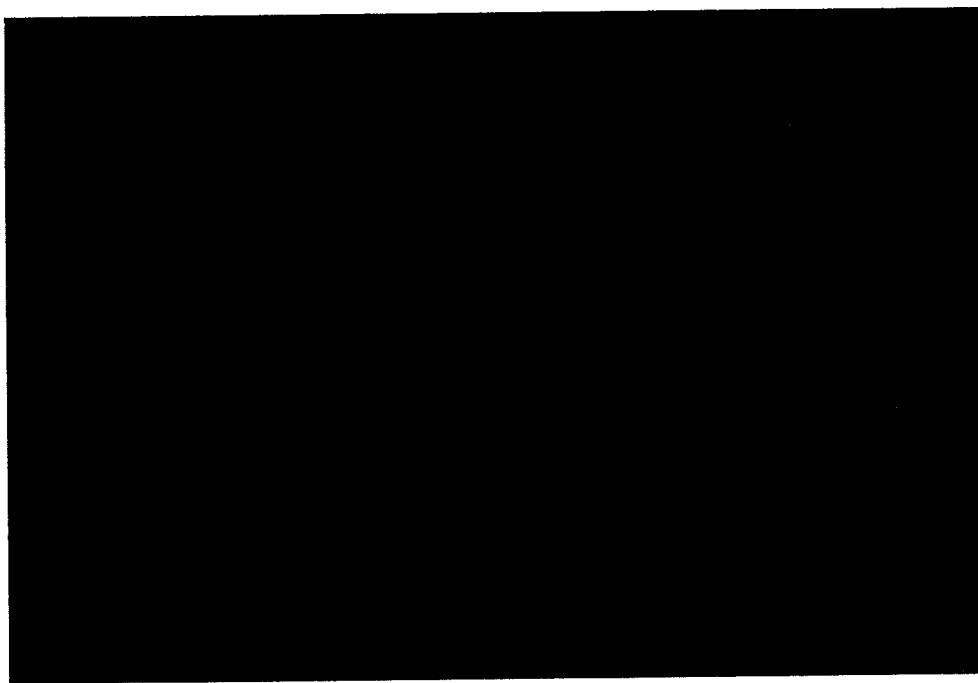


(b)

Figure 9. Micrograph of sample S89-2Ma depicting a homogeneous cement paste. Fluorescence 2.7×3.9 mm. (a) A weakly developed porous zone can be seen along the coarse aggregate interface at the lower right of the picture. (b) View shows fine cracking which appears to radiate out from the central aggregate particle. The cracks may be shrinkage cracks.

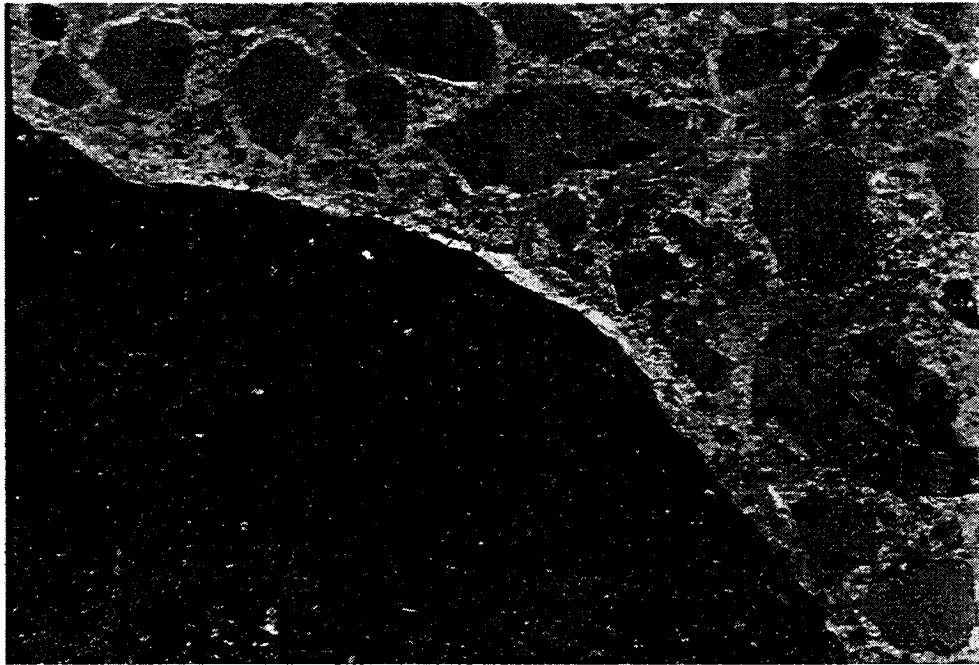


(a)

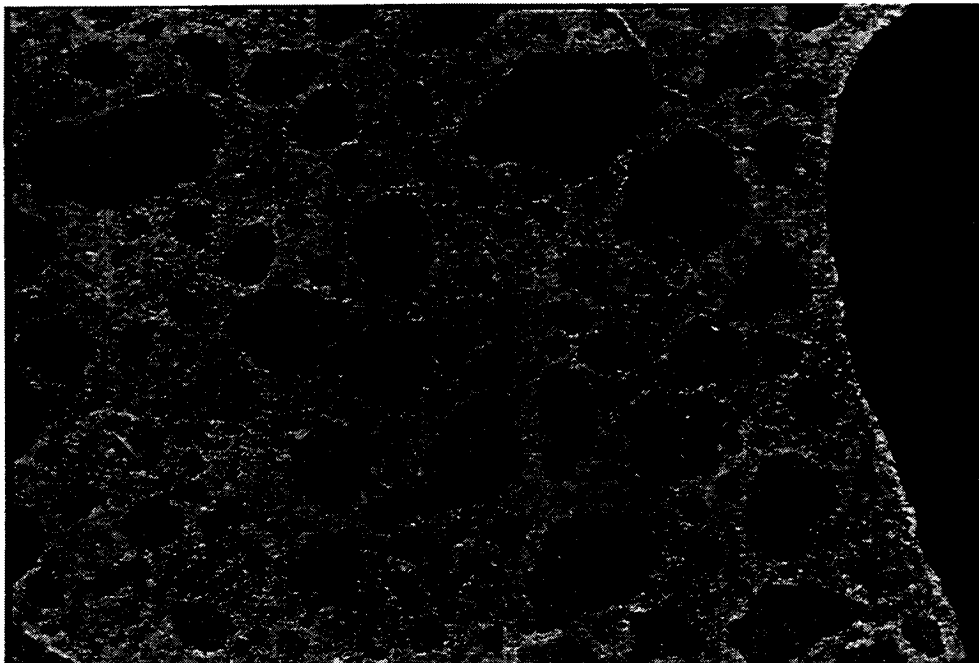


(b)

Figure 10. Micrograph of sample S89-3M28a. Fluorescence. 2.7×3.9 mm. View (a) suggests that the hardened cement paste appears rather homogeneous. View (b) depicts the presence of a spherical air void in the sample. Fine cracks are seen radiating from the void. It is not clear which mechanisms have caused the microcracks.



(a)



(b)

Figure 11. Micrograph of sample S89-4M28a. Fluorescence. 2.7×3.9 mm. View (a) shows that the interface between the coarse aggregate particle to the lower left and the bulk cement paste is dominated by a porous zone. View B suggests that the cement paste, which has an average w/c ratio around 0.46, is homogeneous.

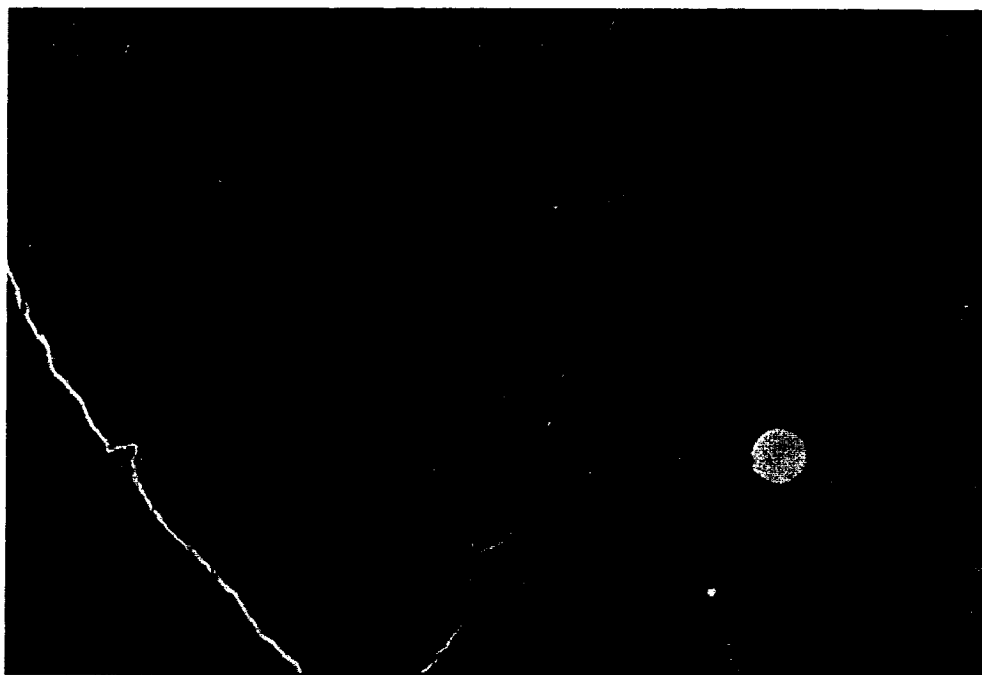


Figure 12. Micrograph of sample S89-5Mb. A coarse aggregate particle (lower left). Note the porous zone between the aggregate and the bulk cement paste. Also note the varying porosity of the cement paste. Fluorescence. 2.7×3.9 mm.

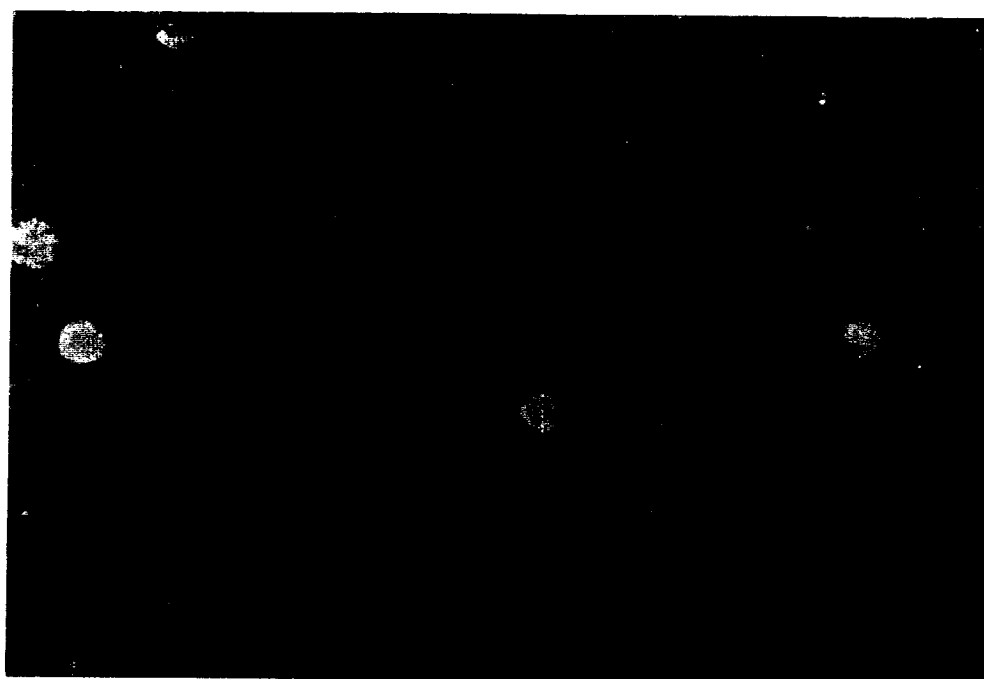


Figure 13. Micrograph of sample S89-6Mb. This thin section illustrates a concrete with practically no paste-aggregate porosity. Fluorescence. 2.7×3.9 mm.

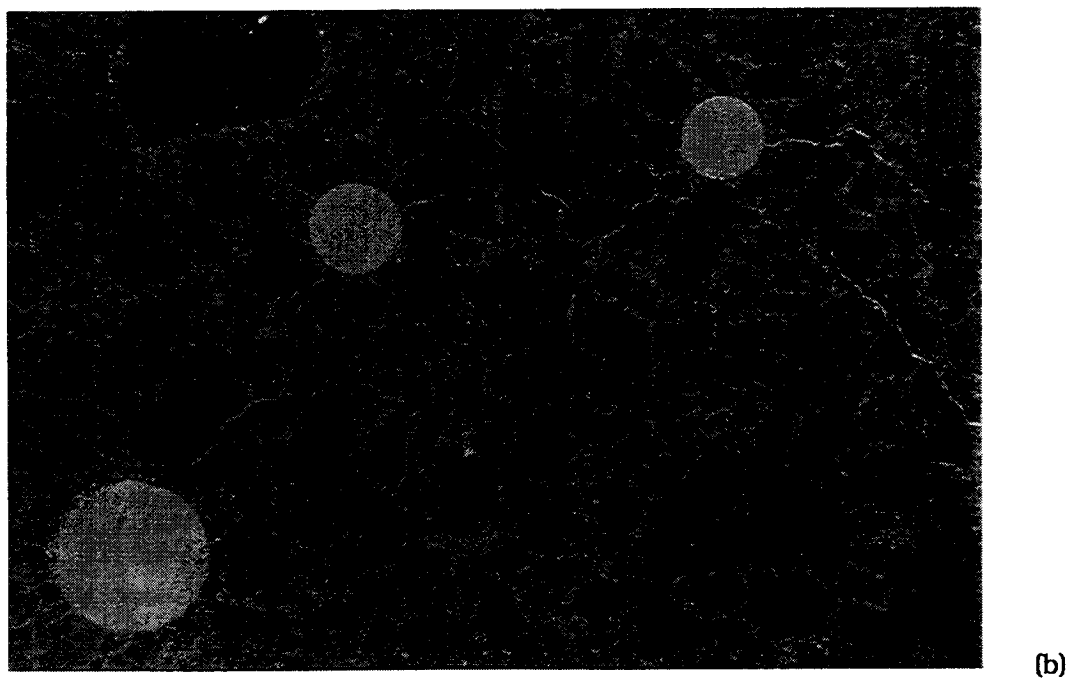
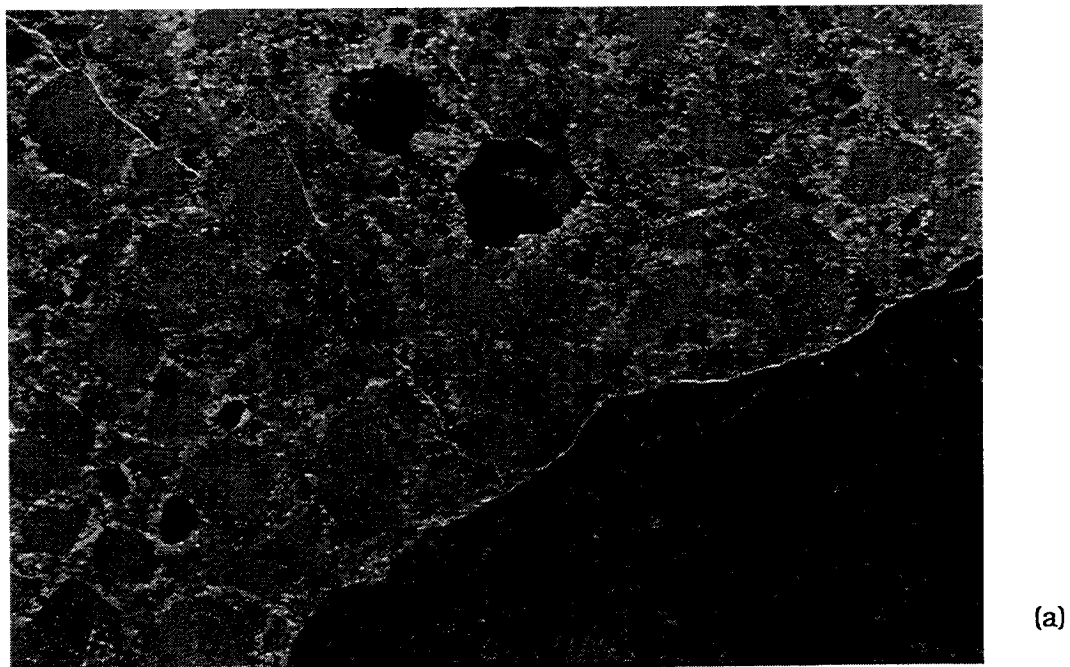
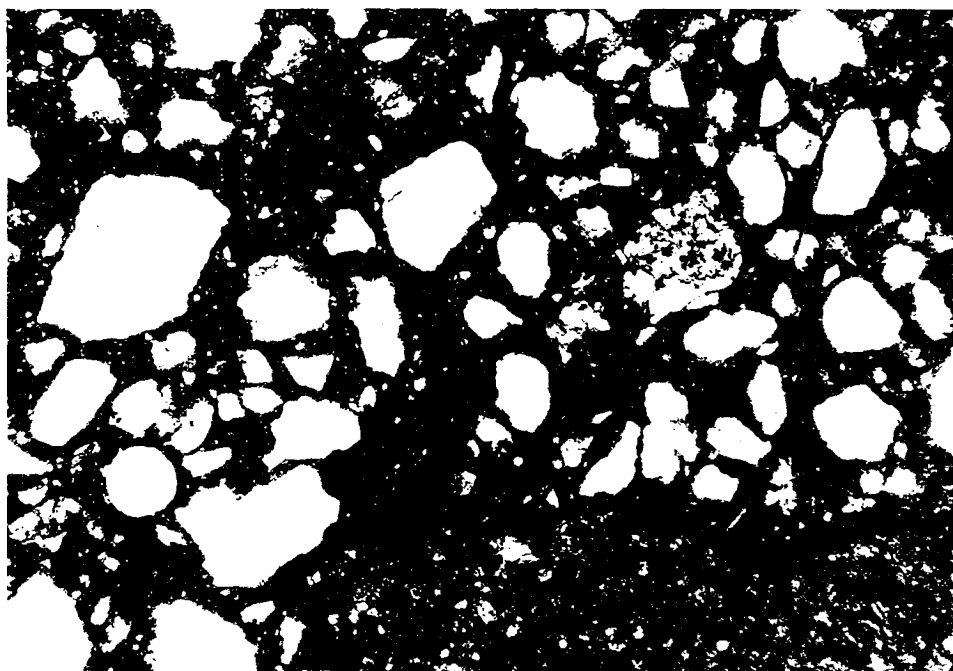
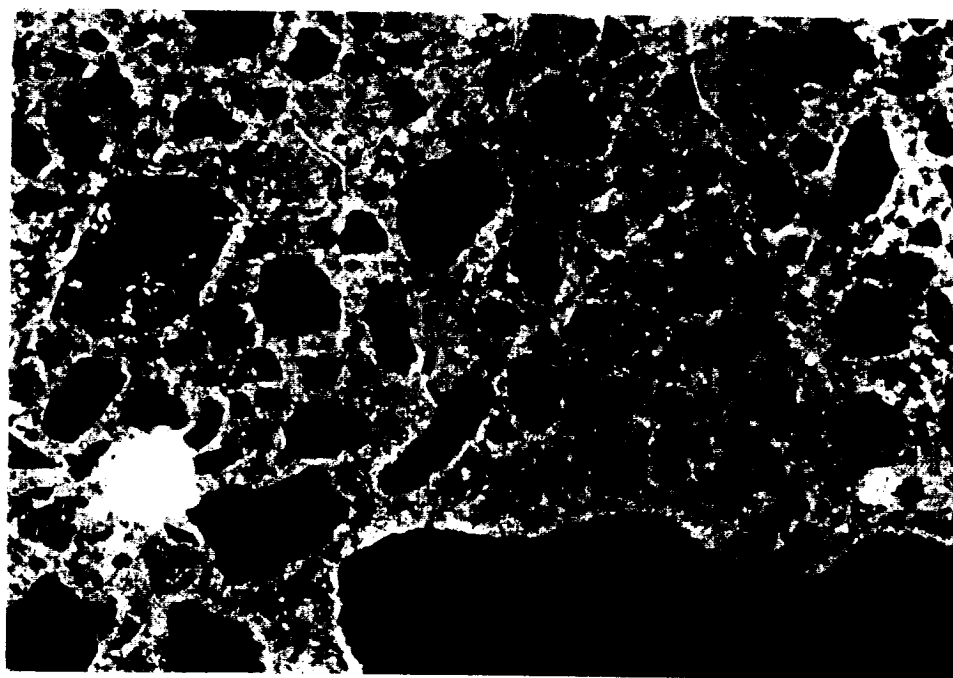


Figure 14. Micrograph of sample S89-7Mb. Fluorescence. 2.7×3.9 mm. View (a) shows a weakly developed porous zone at the interface between the cement paste and the coarse aggregate particle at the lower right. Also note the varying porosity of the hardened cement paste. View (b) depicts the distribution of microcracks radiating from the air voids. It is not clear which mechanism has caused the microcracks.

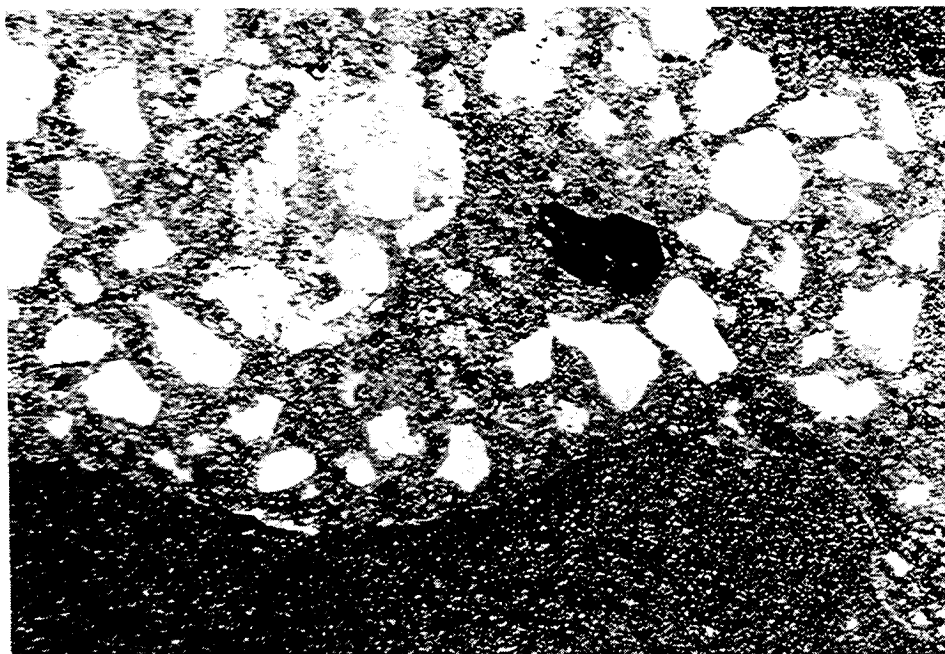


(a)

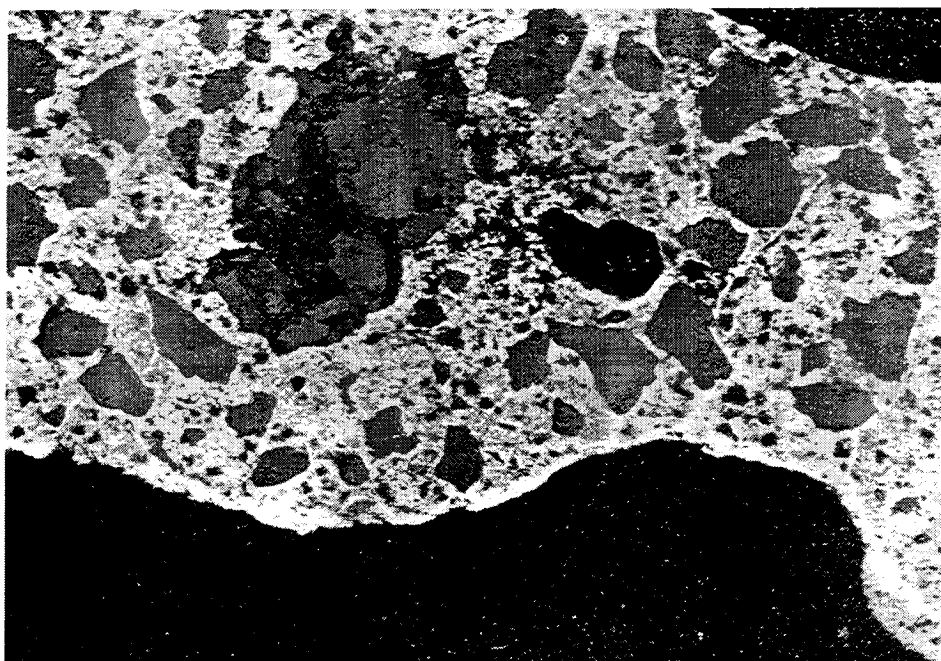


(b)

Figure 15. Micrograph of sample S89-8. Field of view: 3.9×2.7 mm. View (a) represents image in ordinary light. View (b) represents a micrograph of the same area recorded in fluorescent light. Note the general absence of microcracks and paste/aggregate porosity.

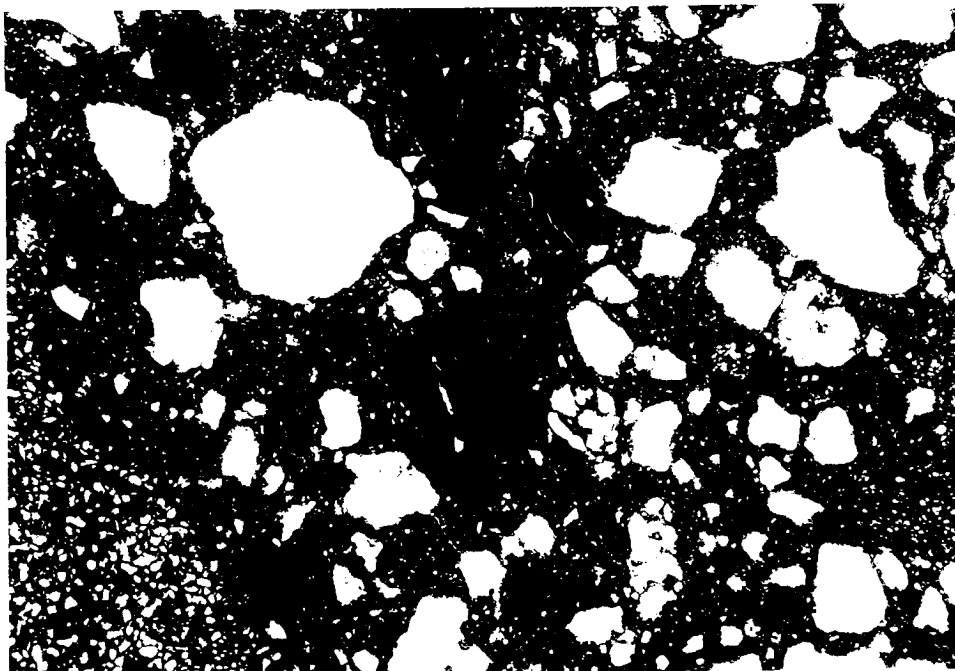


(a)

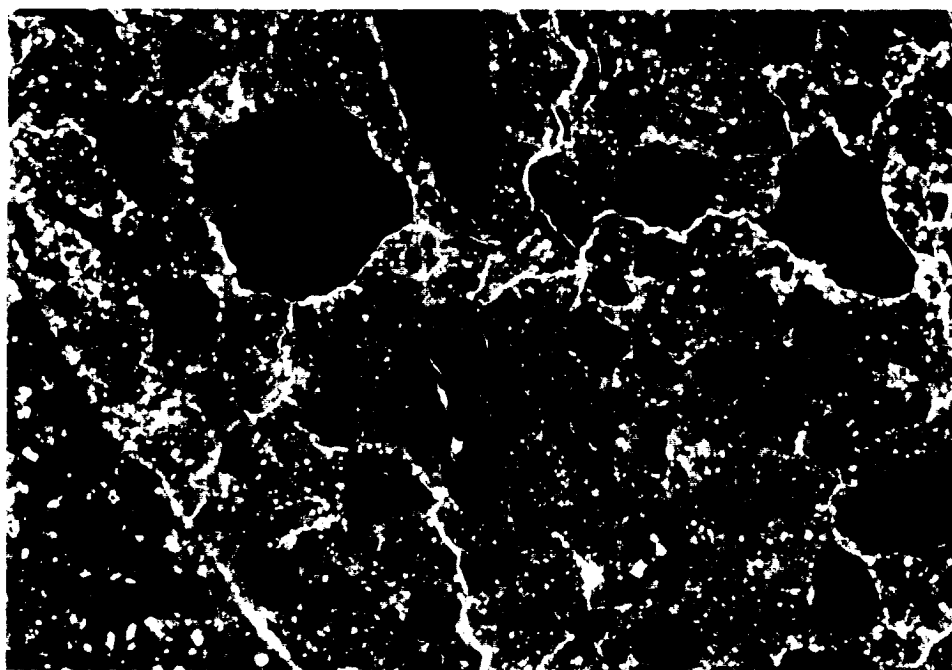


(b)

Figure 16. Micrograph of sample S89-9. Field of view: 3.9×2.7 mm. View (a) represents the appearance of the sample in ordinary light. View (b) represents a micrograph of the same area recorded in fluorescent light.

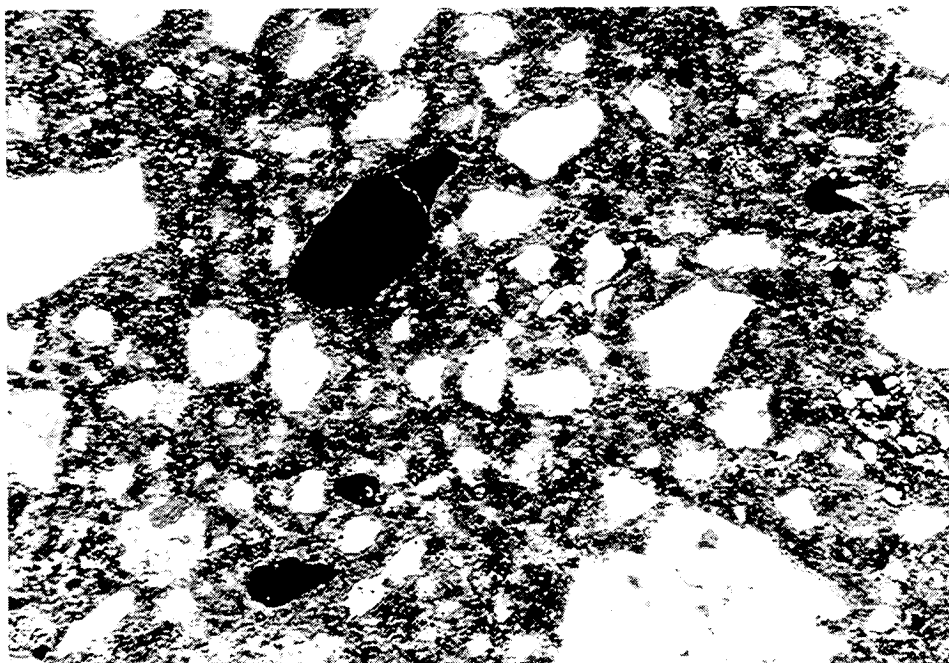


(a)

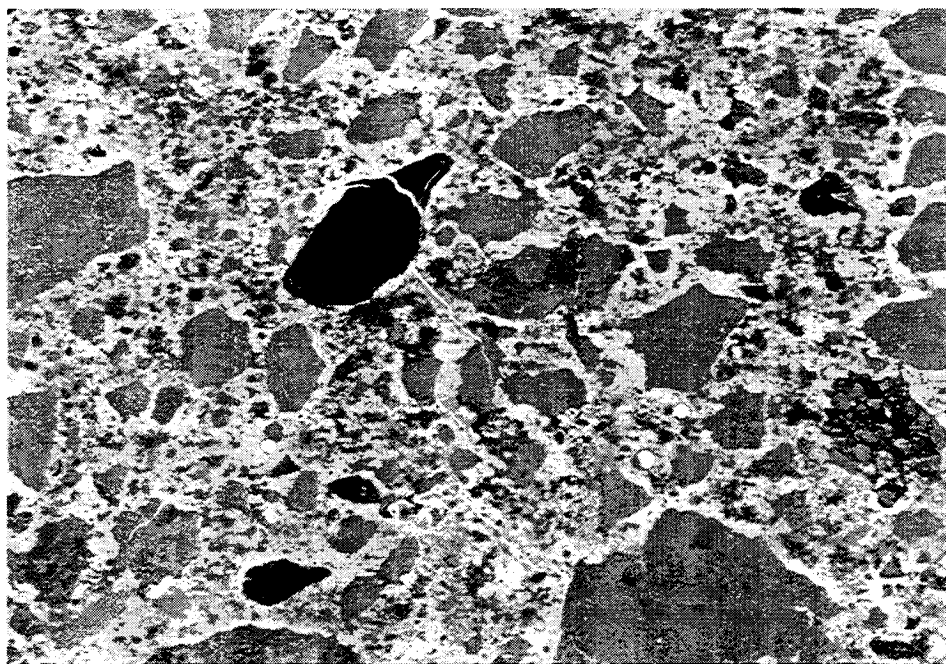


(b)

Figure 17. Micrograph of sample S89-10. Field of view: 3.9×2.7 mm. View (a) is seen in thin section and ordinary light. View (b) is recorded in fluorescent light, depicting the same image as in View (a). Note the grainy appearance of the paste caused by the presence of slag in the cement.

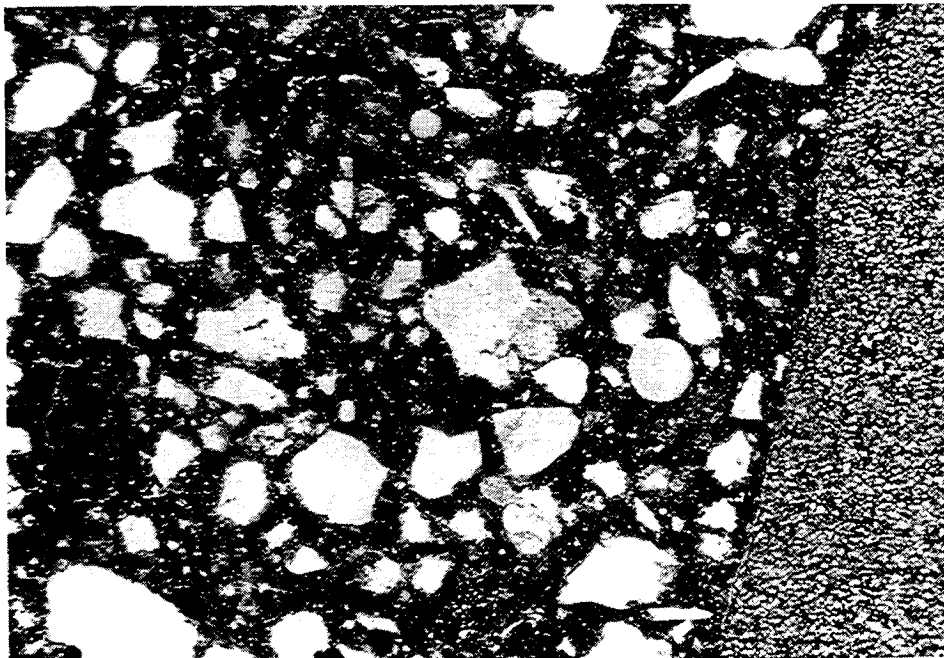


(a)

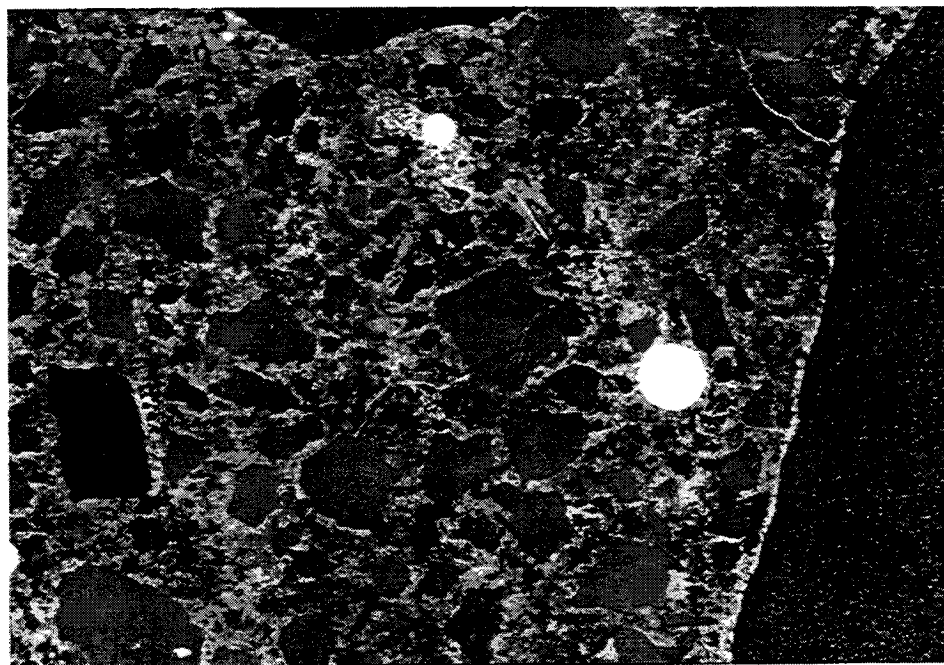


(b)

Figure 18. Micrograph of sample S89-11. Field of view: 3.9×2.7 mm. View (a) depicts the sample in thin section and ordinary light. View (b) gives a micrograph for the same image area recorded in fluorescent light.

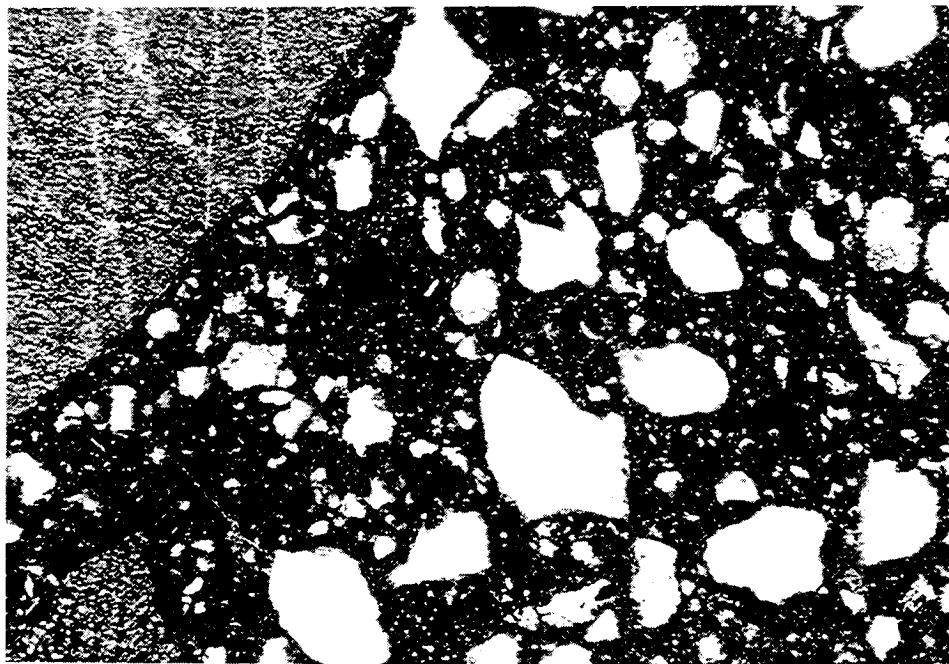


(a)

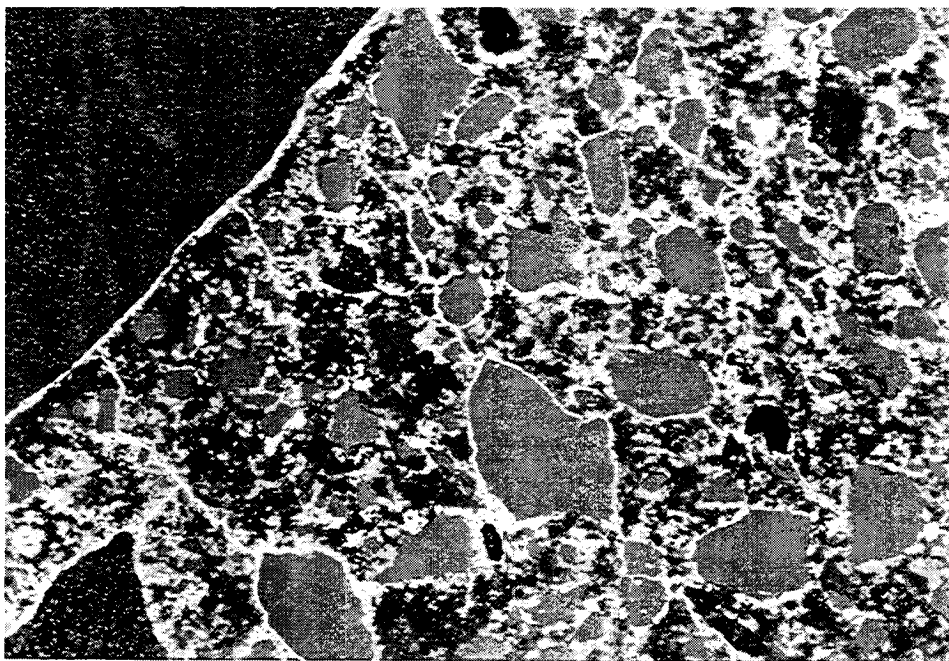


(b)

Figure 19. Micrograph of sample S89-12. Field of view: 3.9×2.7 mm. View (a) gives data as seen in thin section and ordinary light. View (b) is a micrograph for the same image area recorded in fluorescent light.

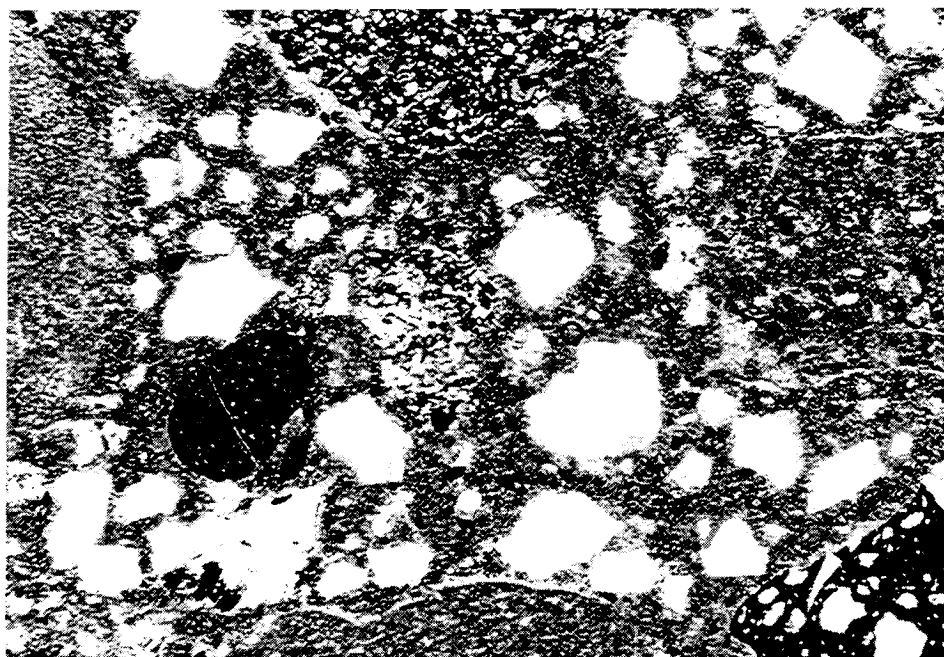


(a)

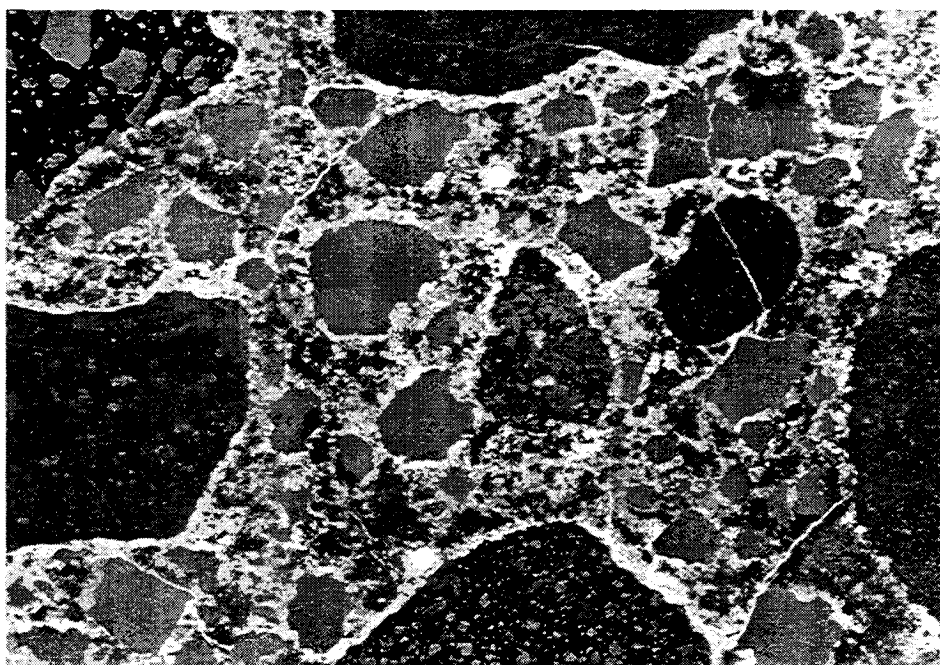


(b)

Figure 20. Micrograph of sample S89-13. Field of view: 3.9×2.7 mm. View (a) is seen in thin section and ordinary light. View (b) is a micrograph of the same image area recorded in fluorescent light.

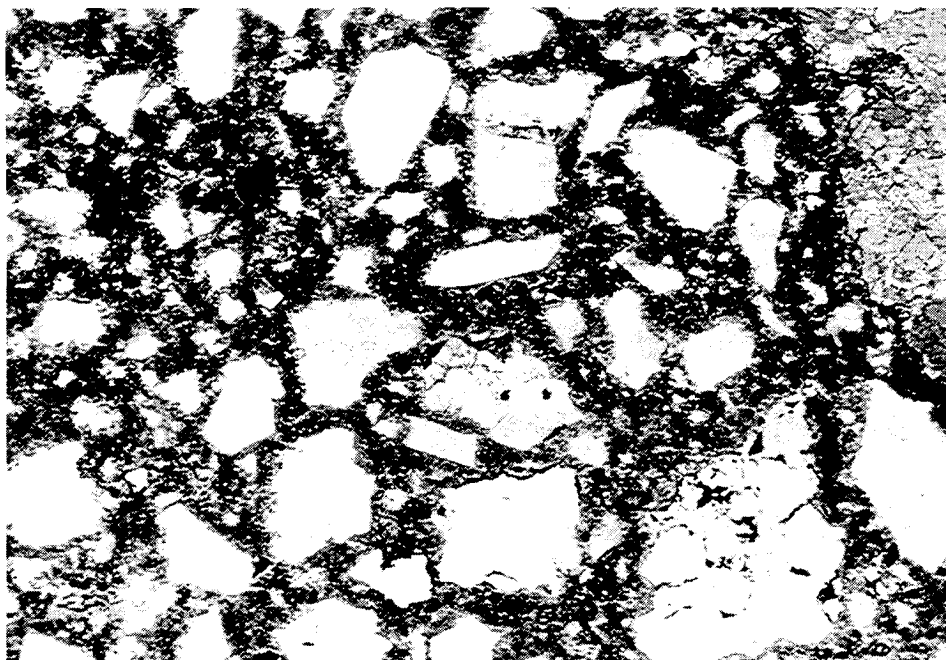


(a)

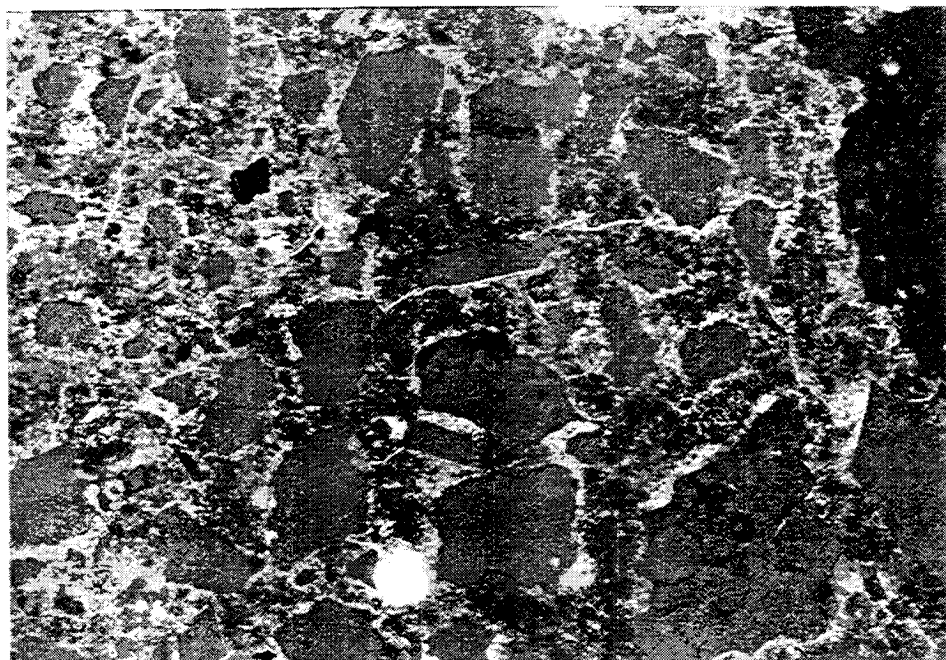


(b)

Figure 21. Micrograph of sample S89-14. Field of view: 3.9×2.7 mm. View (a) depicts its appearance in ordinary light. View (b) represents the same image as View (a), but is recorded in fluorescent light.

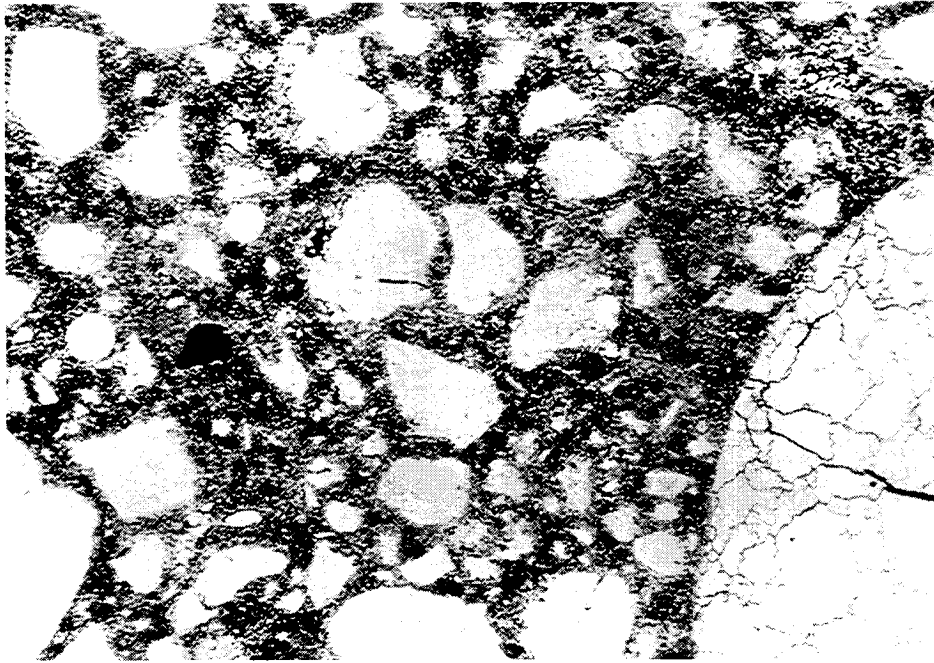


(a)

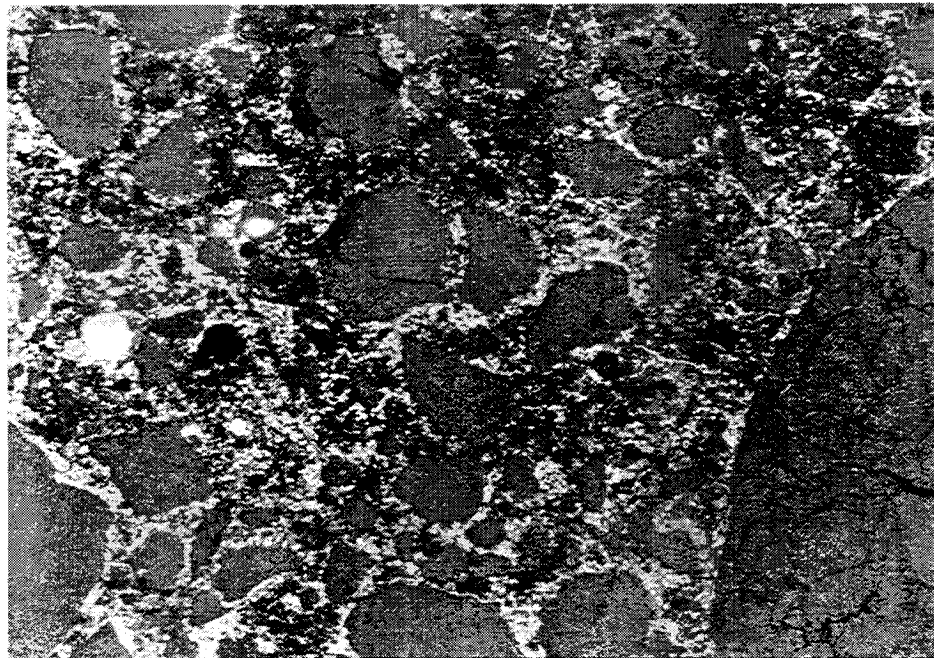


(b)

Figure 22. Micrograph of sample S 89-15. Field of view: 3.9×2.7 mm. View (a) gives details of the sample as seen in ordinary light. View (b) depicts the same image as recorded in fluorescent light.

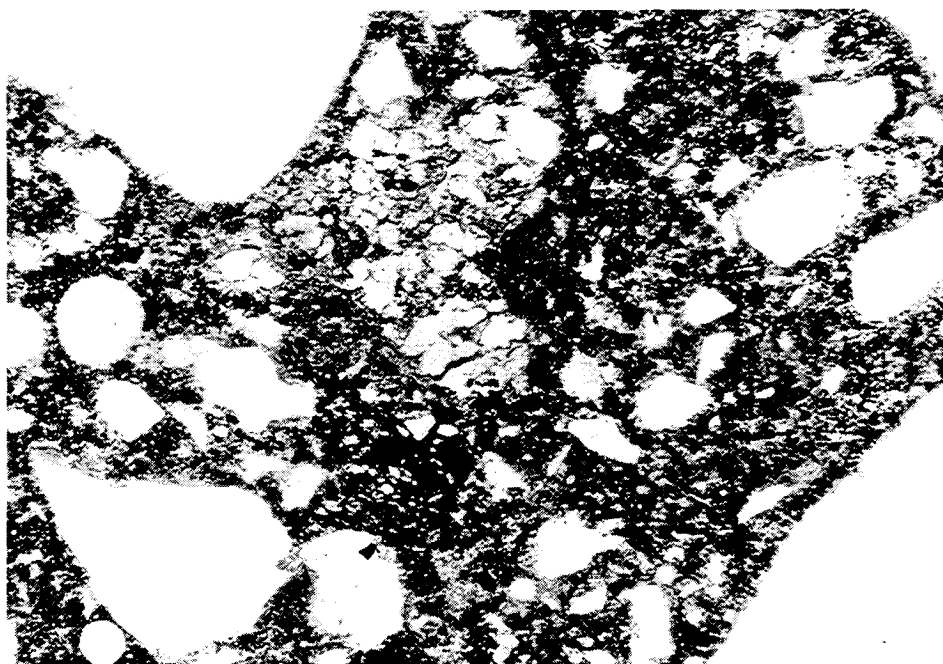


(a)

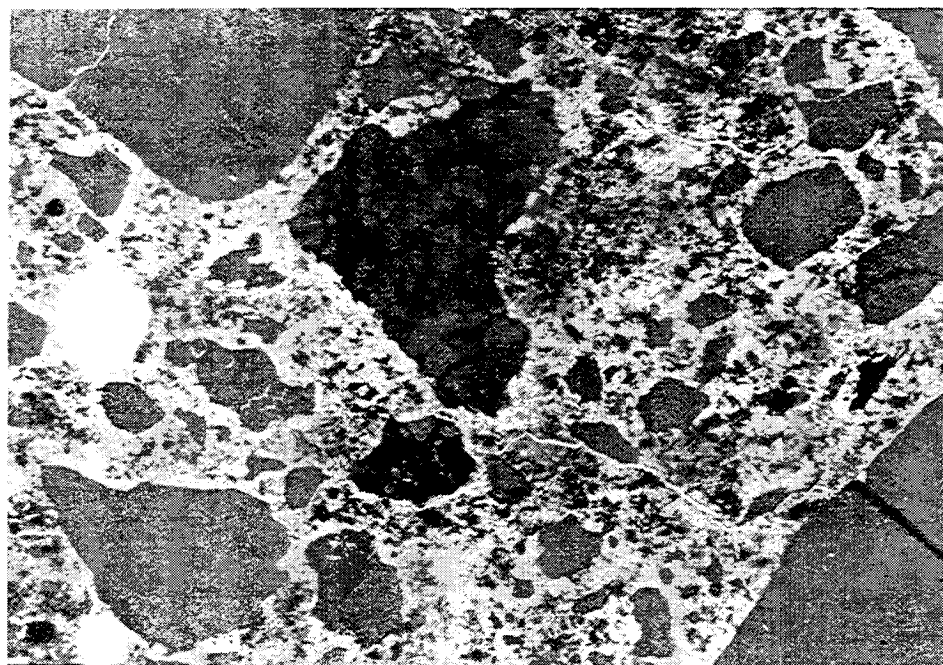


(b)

Figure 23. Micrograph of sample S89-16. Field of view: 3.9×2.7 mm. View (a) represents the sample as seen in thin section recorded in ordinary light. View (b) represents the same sample recorded in fluorescent light.

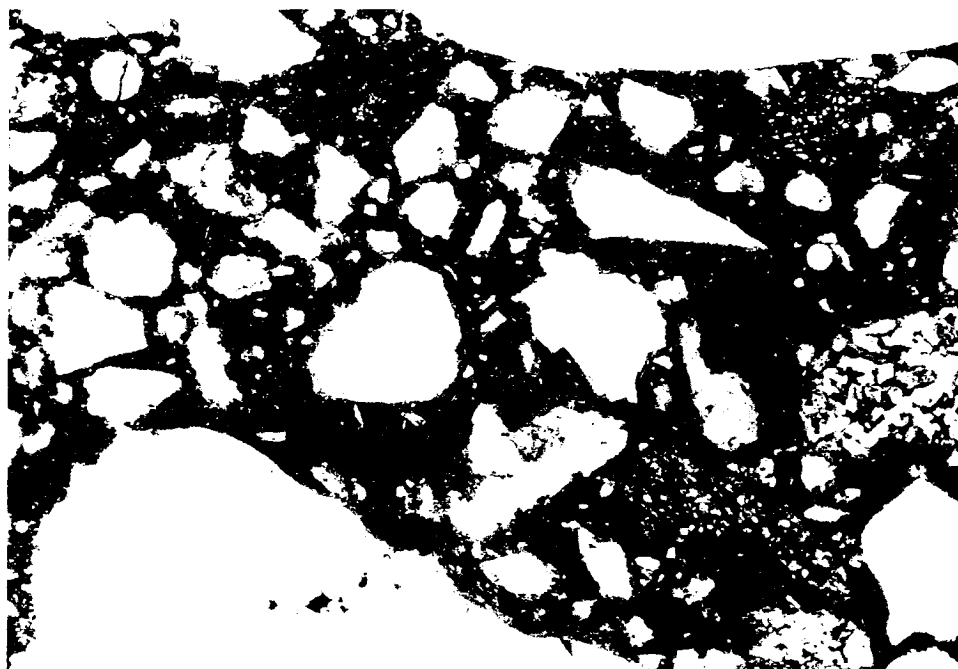


(a)

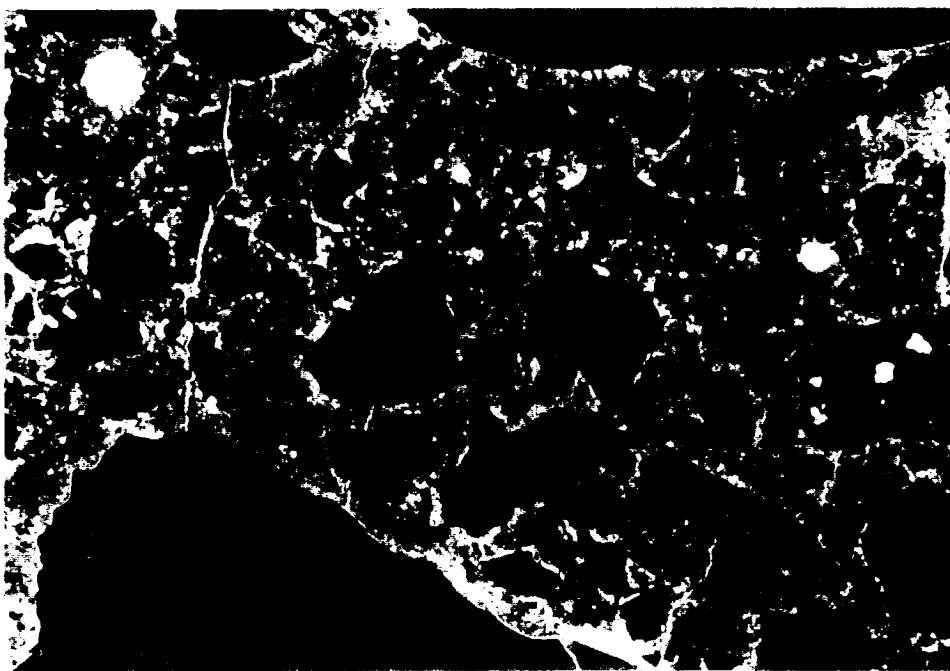


(b)

Figure 24. Micrograph of sample S89-17. Field of view: 3.9×2.7 mm. View (a) represents the sample as seen in thin section and ordinary light. View (b) represents a micrograph of the same area recorded in fluorescent light.

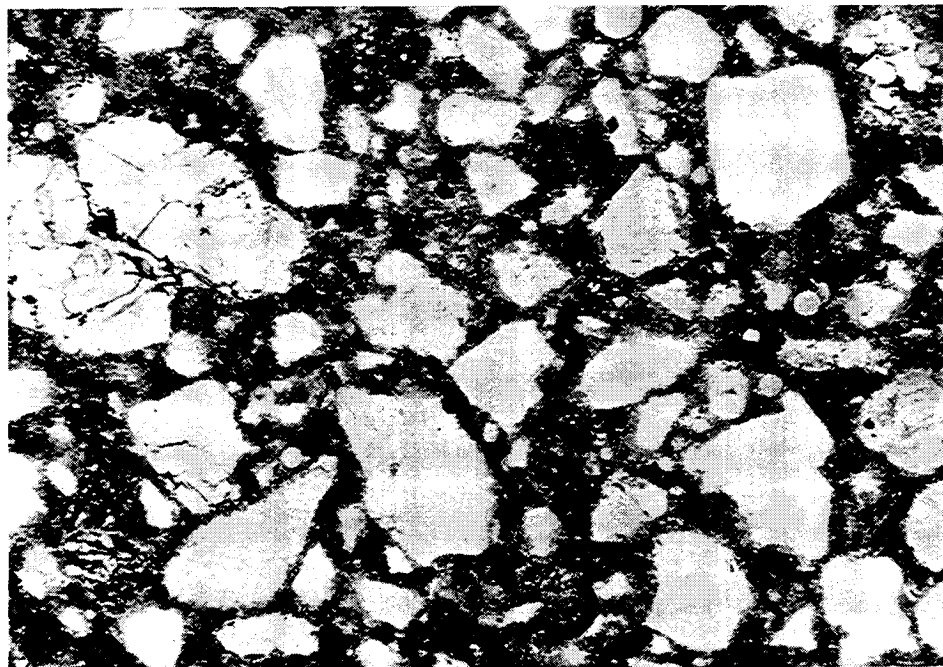


(a)

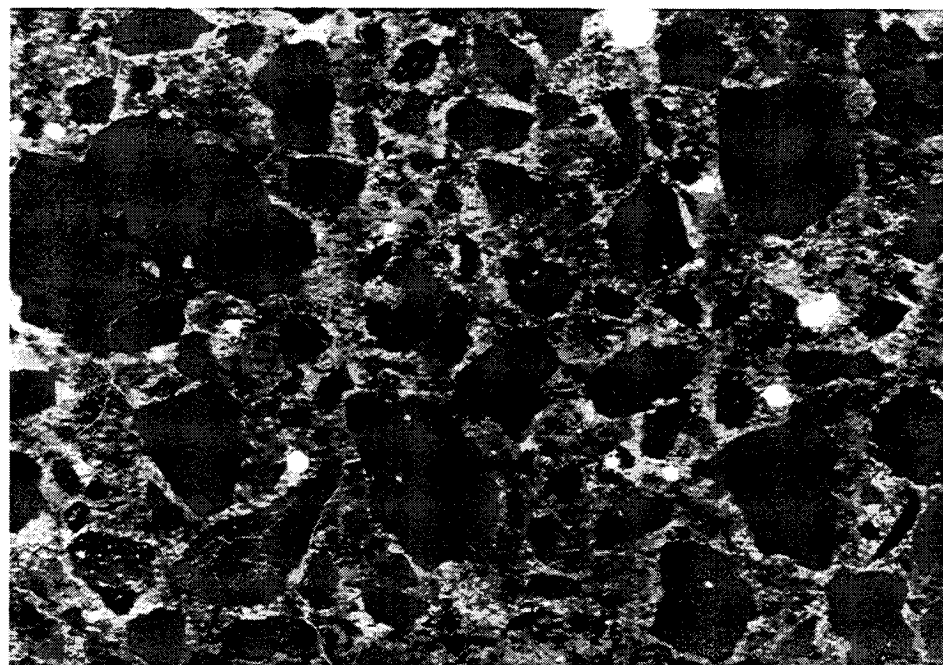


(b)

Figure 25. Micrograph of sample S89-18. Field of view: 3.9×2.7 mm. View (a) depicts the sample as seen in thin section and ordinary light. View (b) represents a micrograph of the same area recorded in fluorescent light.



(a)



(b)

Figure 26. Micrograph of sample S89-19. Field of view: 3.9×2.7 mm. View (a) represents the sample as seen in thin section and ordinary light. View (b) represents the same sample recorded in fluorescent light.

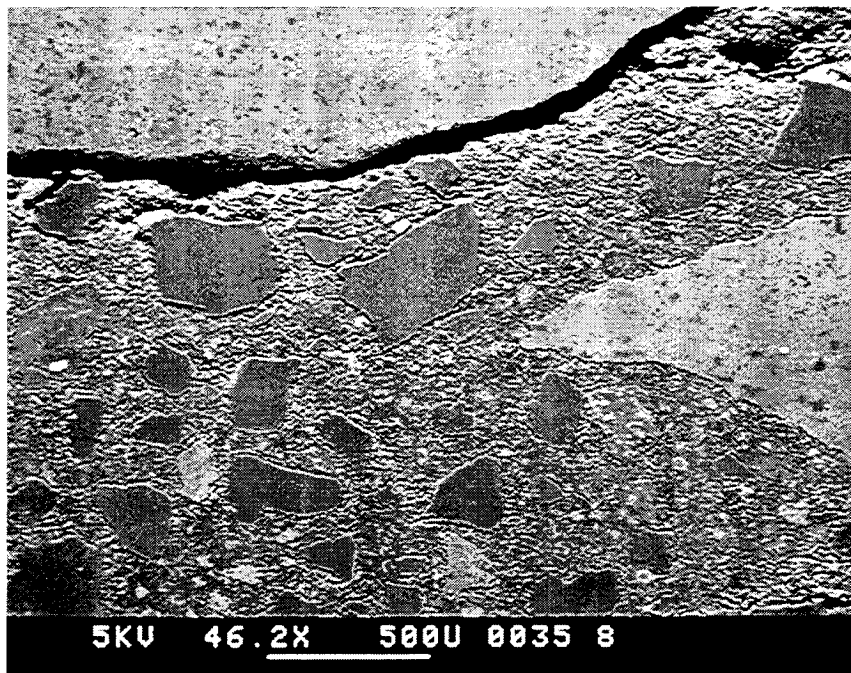


Figure 27. SEM electron backscatter photographs of polished sections of S89-9 (upper) and S89-8 (lower) samples. The higher relief observed in the upper photo is attributed to lower matrix strength.



Figure 28. SEM electron backscatter photographs of polished sections of S89-5 (upper) and S89-4 (lower) samples. Once again, higher relief observed in the upper photo occurred during polishing, reflecting relative matrix weakness.

Appendix B

Tables

Table 1

SNRP-MICROSTRUCTURE C201 microscopy, concrete samples S89-1 - S89-19													
CONCRETE	S89-1	S89-2	S89-3	S89-4	S89-5	S89-6	S89-7						
lbs	32.2	34.2	36.21	36.2	28.29	28.29	28.29						
fine_agg.	51.77	37.05	57.1	75.7	48.56	73.32	89.2						
(#67 limestone)													
coarse_agg.	93.4	106.26	80.55	61.26	106.27	80.55	64.09						
min. adm.													
water	15.13	17.01	17.02	17.02	13.3	13.29	13.3						
Chemical adm.													
density lbs/c.yard	148.35	152.16	149.13	146.15	151.76	149.42	147.74						
Air %	1.5	0.8	0.8	1.8	1.2	2	2.8						
28 days MPa (feret)													
w/c	0.47	0.47	0.47	0.47	0.47	0.47	0.47						
u/filler	0.47	0.47	0.47	0.47	0.47	0.47	0.47						
Slump inch	3.25	2.5	3.5	2	2.75	3.5	3.5						
yield stress	2.8718	4.1496	2.4752	3.1638	4.936	5.1293	5.2323						
viscosity	0.7721	1.2174	0.982	0.7679	0.9803	0.7207	1.27						
Coulomb (RCPT)	1000	253	432	666	253	360	410						
MICROSCOPY													
Coarse agg.													
Volume fraction	0.541	0.552	0.459	0.459	0.566	0.563	0.339						
PI 1/mm	0.1287	0.1609	0.1471	0.0966	0.207	0.138	0.097						
SV 1/mm	0.2574	0.3218	0.2942	0.1932	0.414	0.276	0.194						
lambda mm	7.13	5.57	7.36	11.20	4.00	6.33	13.63						
Cracks													
PI 1/mm	0.049	0.136	0.072	0.07	0.225	0.098	0.137						
L mm	6.65	3.29	7.51	7.73	1.04	4.46	4.82						
epallon	0.2	0.5	0.05	0.5	0.3	0	0.2						
Sv.cracks 1/mm	0.30	0.61	0.27	0.26	1.09	0.45	0.41						

Table 1 ctd.

SHRP MICROSTRUCTURE C201 Microscopy concrete samples S89-1 - S89-19													
CONCRETE	S89-8	S89-9	S89-10	S89-11	S89-12	S89-13	S89-14						
lbs	32.25	24.81	22.32	31.63	31.63	36.42	12.38						
vol. fract	0.127	0.127	0.127	0.080	0.111	0.112	0.119						
fine aggr.	57.02	36.77	60.12	59.62	60.45	59.93	19.91						
							(#B limestone)						
coarse aggr.	93.04	71.85	107.76	107.76	107.76	107.76	35.4						
min. adm.													
water	13.54	13.15	17.49	17.08	15.94	17.49	5.82						
	Mighty 150					Mighty 150							
Chemical admix.	0.32					0.2							
density lbs/c.yard	152.98	148.84	149.52		152.21	150.33	148.79						
Air %	1	0.6	1.2	1.2	1.5	1.3	1.8						
28 days MPa (feret)													
w/c	0.42	0.53	0.76	0.54	0.50	0.51	0.47						
w/filler	0.42	0.53	0.47	0.45	0.42	0.47	0.47						
Slump inch	4	5											
field stress	3.569	1.5874											
viscosity	1.6534	0.7558											
Coulomb (RCPI)	745	1015	347	410	540	60							
MICROSCOPY													
Coarse agg. reg.													
Volume	0.448	0.486	0.486	0.624	0.532	0.587	0.551						
PI 1/mm	0.21	0.358	0.216	0.172	0.16	0.168	0.333						
SV 1/mm	0.42	0.676	0.428	0.344	0.28	0.336	0.666						
lenticle mm	5.26	3.04	4.80	4.37	6.69	4.92	2.70						
Cracks													
PI 1/mm	0.18	0.04	0.251	0.06	0.12	0.455	0.365						
l mm	3.07	12.65	2.05	6.27	3.90	0.91	4.28						
epitall	0.3	0.1	0.51	0.2	0.32	0.3	0.13						
Sv cracks 1/mm	0.65	0.16	0.98	0.32	0.51	2.20	0.47						

Table 1 ctd.

SNAP-MICROSTRUCTURE C201 Microscopy concrete samples S89-1 - S89-19									
CONCRETE	S89-15	S89-16	S89-17	S89-18	S89-19				
	lbs	lbs	vol. fract	vol. fract	vol. fract	lbs	vol. fract	lbs	vol. fract
cement	37.14	12.38	0.128	0.128					
fine_agg.	59.73	19.91	0.248	0.248					
	(#67 silica)								
coarse_agg.	105.78	35.5	0.435						
min. adm.									
water	17.46	5.82	0.190						
Chemical admis.									
density lbs/c.yard	147.93	148.84							
Air %	1.6	2							
28 days MPa (feret)			41.2	40.2					
w/c	0.47	0.47							
w/filler	0.47	0.47							
slump_inch									
yield stress									
viscosity									
Coulomb (RCPI)									
MICROSCOPY									
Coarse_aggreg.									
Volume	0.578	0.532	0.52	0.45	0.26				
pl 1/mm	0.177	0.43	0.191	0.191	0.159				
SV 1/mm	0.354	0.86	0.382	0.382	0.318				
lambda mm	4.77	2.18	5.03	5.76	9.31				
Cracks									
pl 1/mm	0.08	0.13	0.11	0.11	0.11				
L mm	5.28	3.60	4.36	5.00	6.73				
epsilon	0.15	0.18	0.35	0.33	0.2				
SV_cracks 1/mm	0.38	0.56	0.46	0.40	0.30				

Table 2. Concrete Mix No. S89-1Ma.

Recipe		
	Cement (Keystone)	32.20 Pounds
	Lycoming Sand (PTM 616)	51.77 Pounds
	Limestone Aggregate	93.40 Pounds
	Water	15.13 Pounds
	Water/Cement Ratio (calc)	0.47
Microstructure	Scale	
Cracks > 0.1 mm	0	
Cracks < 0.1 mm	1	A few microcracks in paste.
		Average intercept: 1.45 cm Specific surface of crack planes: $1.38 \text{ cm}^2/\text{cm}^3$
Paste/aggregate cracks	1-2	Occasionally porous zones and cracking around several limestone coarse aggregate particles.
		Mean free distance: 0.72 cm Specific aggr. surface: $5.60 \text{ cm}^2/\text{cm}^3$ Interface with porosity: 20% or $1.11 \text{ cm}^2/\text{cm}^3$
Coarse agg. distribution	1	
Fine agg. distribution	0-1	
Cement paste distribution		
macro	1	
micro	1	
Entrapped air	0	
w/c measured		0.46 measured as an average over entire thin section

Table 3. Concrete Mix No. S89-2Ma.

Recipe

Cement (Keystone)	36.20 Pounds
Lycoming Sand (PTM 616)	37.05 Pounds
Limestone Aggregate	106.25 Pounds
Water	17.01 Pounds
Water/Cement Ratio (calc)	0.47

Microstructure

Scale

Cracks > 0.1 mm	0	
Cracks < 0.1 mm	1	A few microcracks in paste.
		Average intercept: 0.74 cm Specific surface of crack planes: $2.72 \text{ cm}^2/\text{cm}^3$
Paste/aggregate cracks	1-2	Porous zones and cracking around several limestone coarse aggregate particles
		Mean free distance: 0.56 cm Specific aggr. surface: $7.18 \text{ cm}^2/\text{cm}^3$ Interface with porosity: 50% or $3.59 \text{ cm}^2/\text{cm}^3$
Coarse agg. distribution	1	
Fine agg. distribution	0-1	
Cement paste distribution		
macro	2	
micro	1	
Entrapped air	0	
w/c measured		0.46 measured as an average over entire thin section

Table 4. Concrete Mix No. S89-3M28a.

Recipe		
	Cement (Keystone)	36.21 Pounds
	Lycoming Sand (PTM 616)	57.10 Pounds
	Limestone Aggregate	80.55 Pounds
	Water	17.02 Pounds
	Water/Cement Ratio (calc)	0.47
Microstructure	Scale	
Cracks > 0.1 mm	0	
Cracks < 0.1 mm	1	A few microcracks in paste.
		Average intercept: 1.39 cm
		Specific surface of crack planes: $1.44 \text{ cm}^2/\text{cm}^3$
Paste/aggregate cracks	1-2	Porous zones and cracking around several limestone coarse aggregate particles.
		Mean free distance: 0.73 cm
		Specific aggr. surface: $5.44 \text{ cm}^2/\text{cm}^3$
		Interface with porosity: 5% or $0.27 \text{ cm}^2/\text{cm}^3$
Coarse agg. distribution	1	
Fine agg. distribution	0-1	
Cement paste distribution		
macro	1	
micro	1-1	
Entrapped air	0	
w/c measured		0.46 measured as an average over entire thin section

Table 5. Concrete Mix No. S89-4M28a.

Recipe

Cement (Keystone)	36.20 Pounds
Lycoming Sand (PTM 616)	75.70 Pounds
Limestone Aggregate	61.26 Pounds
Water	17.02 Pounds
Water/Cement Ratio (calc)	0.47

Microstructure

Scale

Cracks > 0.1 mm	0	
Cracks < 0.1 mm	1	A few microcracks in paste.
		Average intercept: 1.43 cm Specific area of crack planes: 1.40 cm ² /cm ³
Paste/aggregate cracks	1-2	Porous zones and cracking around several limestone coarse aggregate particles.
		Mean free distance: 1.12 cm Specific aggr. surface: 3.57 cm ² /cm ³ Interface with porosity: 30% or 1.07 cm ² /cm ³
Coarse agg. distribution	1	
Fine agg. distribution	0-1	
Cement paste distribution		
macro	1	
micro	0-1	
Entrapped air	0	
w/c measured		0.46 measured as an average over entire thin section

Table 6. Concrete Mix No. S89-5Mb.

Recipe

Cement (Keystone)	28.29 Pounds
Lycoming Sand (PTM 616)	48.56 Pounds
Limestone Aggregate	106.27 Pounds
Water	13.30 Pounds
Water/Cement Ratio (calc)	0.47

Microstructure

Scale

Cracks > 0.1 mm	0	
Cracks < 0.1 mm	2	Several microcracks in paste.
		Average intercept: 0.45 cm Specific area of crack planes: $4.55 \text{ cm}^2/\text{cm}^3$
Paste/aggregate cracks	2-3	Porous zones and cracking around several limestone coarse aggregate particles.
		Mean free distance: 0.40 cm Specific aggr. surface: $10.10 \text{ cm}^2/\text{cm}^3$ Interface with porosity: 30% or $3.03 \text{ cm}^2/\text{cm}^3$
Coarse agg. distribution	0-1	
Fine agg. distribution	0-1	
Cement paste distribution		
macro	2	Area with more dense paste in one side of thin section.
micro	2	Some clotting in paste.
Entrapped air	0	
w/c measured		0.42 measured as an average over entire thin section

Table 7. Concrete Mix No. S89-6Mb.

Recipe

Cement (Keystone)	28.29 Pounds
Lycoming Sand (PTM 616)	73.32 Pounds
Limestone Aggregate	80.55 Pounds
Water	13.29 Pounds
Mighty 150 SPL	0.42
Water/Cement Ratio (calc)	0.47

Microstructure**Scale**

Cracks > 0.1 mm	0	
Cracks < 0.1 mm	1	A few microcracks in paste.
		Average intercept: 1.18 cm Specific area of crack planes: $1.70 \text{ cm}^2/\text{cm}^3$
Paste/aggregate cracks	2-3	Occasionally cracking around limestone coarse aggregate particles but practically no porosities.
		Mean free distance: 0.63 cm Specific aggr. surface: $6.32 \text{ cm}^2/\text{cm}^3$ Interface with porosity: 0% or $0 \text{ cm}^2/\text{cm}^3$
Coarse agg. distribution	1	
Fine agg. distribution	0-1	
Cement paste distribution		
macro	1	Area with more dense paste in one side of thin section.
micro	1-2	Some clotting in paste.
Entrapped air	0	
w/c measured		0.46 measured as an average over entire thin section

Table 8. Concrete Mix No. S89-7Mb.

Recipe		
	Cement (Keystone)	28.29 Pounds
	Lycoming Sand (PTM 616)	89.20 Pounds
	Limestone Aggregate	64.09 Pounds
	Water	13.30 Pounds
	Mighty 150 SPL	0.63
	Water/Cement Ratio (calc)	0.47
Microstructure	Scale	
Cracks > 0.1 mm	0	
Cracks < 0.1 mm	1	A few microcracks in paste.
		Average intercept: 0.74 cm Specific area of crack planes: 2.70 cm ² /cm ³
Paste/aggregate cracks	1	Occasionally porous zones and cracking around limestone coarse aggregate particles.
		Mean free distance: 1.36 cm Specific aggr. surface: 2.93 cm ² /cm ³ Interface with porosity: 20% or 0.59 cm ² /cm ³
Coarse agg. distribution	1	
Fine agg. distribution	0-1	
Cement paste distribution		
macro	1	Area with more dense paste in one side of thin section.
micro	1-2	Some clotting in paste.
Entrapped air	0	
w/c measured		0.46 measured as an average over entire thin section

Table 9. Concrete Mix No. S89-8.

Recipe

Cement (Keystone)	32.25	Pounds
Lycoming Sand (PTM 616)	57.02	Pounds
Limestone Aggregate	93.04	Pounds
Water	13.54	Pounds
Mighty 150 SPL.	0.32	Pounds
Water/Cement Ratio (calc)	0.42	

Inhomogeneity

Coarse agg. distribution	1
Fine agg. distribution	0/1
Cement paste	
macro	1
micro	1
Entrapped air	0
w/c measured	0.45

Coarse Aggregate

P ₁	mm ⁻¹	0.21
S _v = 2xP ₁	mm ⁻¹	0.42
Lambda	mm ⁻¹	5.26

Microcracks

P ₁	mm ⁻¹	0.18
L	mm	3.07
Epsilon		0.30

Table 10. Concrete Mix No. S89-9.

Recipe			
	Cement (Keystone)	24.81	Pounds
	Lycoming Sand (PTM 616)	36.57	Pounds
	Limestone Aggregate	71.85	Pounds
	Water	13.15	Pounds
	Water/Cement Ratio (calc)	0.53	
Inhomogeneity			
	Coarse agg. distribution	1	
	Fine agg. distribution	0/1	
	Cement paste		
	macro	1	
	micro	1	
	Entrapped air	0	
	w/c measured	0.45	
Coarse Aggregate			
	P_1	mm^{-1}	0.338
	$S_v = 2 \times P_1$	mm^{-1}	0.676
	Lambda	mm^{-1}	3.04
Microcracks			
	P_1	mm^{-1}	0.04
	L	mm	12.85
	Epsilon		0.10

Table 11. Concrete Mix No. S89-10.

Recipe			
Cement (Keystone)2	2.32	Pounds	
Lycoming Sand (PTM 616)	60.12	Pounds	
Limestone Aggregate	107.78	Pounds	
Newcem Slag	14.88	Pounds	
Water	17.49	Pounds	
Water/Binder Ratio (calc)	0.47		
Inhomogeneity			
Coarse agg. distribution	1		
Fine agg. distribution	0/1		
Cement paste			
macro	1		
micro	1		
Entrapped air	0		
w/c measured	0.35		
Coarse Aggregate			
P ₁	mm ⁻¹	0.214	
S _v = 2xP ₁	mm ⁻¹	0.428	
Lambda	mm ⁻¹	4.80	
Microcracks			
P ₁	mm ⁻¹	0.251	
L	mm	2.05	
Epsilon		0.51	

Table 12. Concrete Mix No. S89-11.

Recipe

Cement (Keystone)	31.61	Pounds
Lycoming Sand (PTM 616)	59.62	Pounds
Limestone Aggregate	107.78	Pounds
Fly Ash Class F	6.33	Pounds
Water	17.08	Pounds
Water/Binder Ratio (calc)	0.47	

Inhomogeneity

Coarse agg. distribution	1
Fine agg. distribution	0/1
Cement paste	
macro	1
micro	1
Entrapped air	0
w/c measured	0.45

Coarse Aggregate

P_1	mm^{-1}	0.172
$S_v = 2 \times P_1$	mm^{-1}	0.344
Lambda	mm^{-1}	4.37

Microcracks

P_1	mm^{-1}	0.06
L	mm	6.27
Epsilon		0.20

Table 13. Concrete Mix No. S89-12.

Recipe

Cement (Keystone)	31.63	Pounds
Lycoming Sand (PTM 616)	60.45	Pounds
Limestone Aggregate	107.78	Pounds
Fly Ash Class C	6.33	Pounds
Water	15.94	Pounds
Water/Binder Ratio (calc)	0.47	

Inhomogeneity

Coarse agg. distribution	1
Fine agg. distribution	0/1
Cement paste	
macro	1
micro	1
Entrapped air	0
w/c measured	0.45

Coarse Aggregate

P_1	mm^{-1}	0.14
$S_v = 2xP_1$	mm^{-1}	0.28
Λ	mm^{-1}	6.69

Microcracks

P_1	mm^{-1}	0.12
L	mm	3.90
Epsilon		0.32

Table 14. Concrete Mix. No. S89-13

Recipe			
Cement (Keystone)		34.42	Pounds
Lycoming Sand (PTM 616)		59.93	Pounds
Limestone Aggregate		107.78	Pounds
Silica Fume		2.79	Pounds
Water		15.13	Pounds
Mighty 150 SPL		0.2	Pounds
Water/Binder Ratio (calc)		0.47	
Inhomogeneity			
Coarse agg. distribution		1	
Fine agg. distribution		0/1	
Cement paste			
macro		1	
micro		1	
Entrapped air		0	
w/c measured		0.45	
Coarse Aggregate			
P_1	mm^{-1}	0.168	
$S_v = 2 \times P_1$	mm^{-1}	0.336	
Λ	mm^{-1}	4.92	
Microcracks			
P_1	mm^{-1}	0.455	
L	mm	0.91	
Epsilon		0.30	

Table 15. Concrete Mix No. S89-14.

Recipe			
Cement (Keystone)		12.38	Pounds
Lycoming Sand (PTM 616)		19.91	Pounds
Limestone Aggregate#8		35.40	Pounds
Water		5.82	Pounds
Water/Cement Ratio (calc)		0.47	
Inhomogeneity			
Coarse agg. distribution		1	
Fine agg. distribution		0/1	
Cement paste			
macro		1	
micro		1	
Entrapped air		0	
w/c measured		0.45	
Coarse Aggregates			
P_1	mm^{-1}	0.333	
$S_v = 2xP_1$	mm^{-1}	0.666	
Lambda	mm^{-1}	2.70	
Microcracks			
P_1	mm^{-1}	0.105	
L	mm	4.28	
Epsilon		0.13	

Table 16. Concrete Mix No. S89-15.

Recipe

Cement (Keystone)	37.14	Pounds
Lycoming Sand (PTM 616)	59.73	Pounds
Siliceous Aggregate#67	105.78	Pounds
Water	17.46	Pounds
Water/Cement Ratio (calc)	0.47	

Inhomogeneity

Coarse agg. distribution	1
Fine agg. distribution	0/1
Cement paste	
macro	1
micro	1
Entrapped air	0
w/c measured	0.45

Coarse Aggregate

P_1	mm^{-1}	0.177
$S_v = 2 \times P_1$	mm^{-1}	0.354
Λ	mm^{-1}	4.77

Microcracks

P_1	mm^{-1}	0.08
L	mm	5.28
Epsilon		0.15

Table 17. Concrete Mix No. S89-16.

Recipe			
Cement (Keystone)		12.38	Pounds
Lycoming Sand (PTM 616)		19.91	Pounds
Limestone Aggregate		35.40	Pounds
Water		5.82	Pounds
Water/Cement Ratio (calc)		0.47	
Inhomogeneity			
Coarse agg. distribution		1	
Fine agg. distribution		0/1	
Cement paste			
macro		1	
micro		1	
Entrapped air		0	
w/c measured		0.45	
Coarse Aggregate			
P_1	mm^{-1}	0.43	
$S_v = 2xP_1$	mm^{-1}	0.86	
Λ	mm^{-1}	2.18	
Microcracks			
P_1	mm^{-1}	0.13	
L	mm	3.60	
Epsilon		0.18	

Table 18. Concrete Mix No. S89-17.

Recipe			
	Cement (Keystone)	20.90	Pounds
	Lycoming Sand (PTM 616)	18.68	Pounds
	Towson Siliceous Aggregate	60.18	Pounds
	Water	9.82	Pounds
	Water/Cement Ratio (calc)	0.47	
Inhomogeneity			
	Coarse agg. distribution	1	
	Fine agg. distribution	1	
	Cement paste		
	macro	1	
	micro	1	
	Entrapped air	0/1	
	w/c measured	0.40 - 0.45	
Coarse aggregate			
	P_l	mm^{-1}	0.191
	$S_v = 2 \times P_l$	mm^{-1}	0.382
	Lambda	mm^{-1}	5.03
Microcracks			
	P_l	mm^{-1}	0.11
	L	mm	4.36
	Epsilon		0.35

Table 19. Concrete Mix No. S89-18.

Recipe				
	Cement (Keystone)		20.90	Pounds
	Lycoming Sand (PTM 616)		32.94	Pounds
	Towson Siliceous Aggregate		45.53	Pounds
	Water		9.83	Pounds
	Water/Cement Ratio (calc)		0.47	
Inhomogeneity				
	Coarse agg. distribution		1	
	Fine agg. distribution		0/1	
	Cement paste			
	macro		1	
	micro		1	
	Entrapped air		0	
	w/c measured		0.35	
Coarse aggregate				
	P_1	mm^{-1}	0.191	
	$S_v = 2 \times P_1$	mm^{-1}	0.382	
	Lambda	mm^{-1}	5.76	
Microcracks				
	P_1	mm^{-1}	0.11	
	L	mm	5.00	
	Epsilon		0.33	

Table 20. Concrete Mix No. S89-19.

Recipe

Cement (Keystone)	20.90	Pounds
Lycoming Sand (PTM 616)	43.67	Pounds
Towson Siliceous Aggregate	34.70	Pounds
Water	9.83	Pounds
Water/Cement Ratio (calc)	0.47	

Inhomogeneity

Coarse agg. distribution	1
Fine agg. distribution	0/1
Cement paste	
macro	1
micro	1
Entrapped air	0
w/c measured	0.35 - 0.40

Coarse aggregate

P_1	mm^{-1}	0.159
$S_v = 2 \times P_1$	mm^{-1}	0.318
Λ	mm^{-1}	9.31

Microcracks

P_1	mm^{-1}	0.11
L	mm	6.73
Epsilon		0.20

Appendix C

Nordtest 677-87

Concrete, Hardened; Water-Cement Ratio

1 (4)

CONCRETE, HARDENED: WATER-CEMENT RATIO

UDC 691.32

Key words: test method, concrete, hardened

1 SCOPE

This NORDTEST method can be applied to estimate the water-cement ratio (W/C ratio) in hardened concrete, using microscopic investigation of thin sections.

2 FIELD OF APPLICATION

The method is applicable for well-hydrated Ordinary Portland Cement (OPC) concrete with or without admixtures such as plasticizers and air-void entraining agents.

The degree of hydration of the tested concrete and the references should be of the same order.

The method is not applicable when fly ash, silica fume and slag are present. In these cases the "equivalent water-cement ratio" is estimated in the same manner as for OPC. It is not possible to estimate the W/C of Polymer Cement Concrete (PCC) or of coloured concrete.

3 REFERENCES

Sandström Matz: Mikroskopisk bedömning av vct i betong. SP-AR 1988:43, Statens provningsanstalt, Borås 1988.

Kristensen J A, Brandt I, Damgård Jensen A: Betons mikrostruktur. Projektrapport, Teknologisk Institut, Taastrup 1988.

NORDTEST: NT BUILD 191, NT BUILD 192, NT BUILD 202

4 DEFINITIONS

Water-Cement Ratio: W/C ratio. The ratio by weight between water and cement in concrete.

Capillary porosity: The number of submicroscopic pores (greater than 50 nm) which can possibly be filled with epoxy resin.

Degree of hydration: The ratio by weight of hydrated cement to the total cement.

Equivalent W/C ratio: The apparent W/C ratio of concrete containing fly ash, silica fume or slag.

5 SAMPLING

If no sampling procedure is described in the test report, sampling is as stated in NT BUILD 191 or NT BUILD 202.

The number of specimens is not stipulated.

6 METHOD OF TESTING

6.1 Principle

The capillary pores in the cement paste are filled with fluorescent epoxy by impregnating the specimen in vacuum. A thin section is then prepared and analyzed in a microscope. The intensity of fluorescence of the cement paste is a function of the capillary porosity. The capillary porosity is a function of the W/C ratio and the degree of hydration. The W/C ratio can therefore be estimated by comparing the thin section of the test sample with a thin section of a reference sample under a microscope.

6.2 Apparatus

6.2.1 For preparation of thin sections

Diamond saw

Drying chamber

Vacuum chamber

Face grinding machine with diamond impregnated disc for coarse surface grinding.

Face grinding disc impregnated with diamonds, of grain size 25 – 30 microns, for final surface grinding.

Epoxy Resin CIBA CEIGY BY 158 or equivalent

Hardener CIBA CEIGY HY 2996 or equivalent

Fluorescent dye DAYGLO HUDSON YELLOW or equivalent, (1 % by weight of the epoxy)

Alcohol

Microscope slide minimum 28 x 48 mm

Cover glass

Canada Balsam or equivalent

Epoxy Low molecular weight

6.2.2 For examination of thin section

Standard polarizing microscope for examination in transmitted light with

Barrier filter 510 – 530 nm

Lenses 2 – 10x

Oculars 10x

Exciter filter BG12, 3 mm or equivalent

6.3 Preparation of samples

6.3.1 Preparation of thin sections

The following procedure is an example of the method of preparation. Other methods can be used as long as a thin section with the same thickness and quality is obtained.

Cutting of the specimen

A specimen of minimum size 40 x 20 x 10 mm, see figure 1, is cut with a diamond saw and glued with epoxy on a microscope slide (working glass). The specimen is then face ground, see figure 1.

Drying the specimen

The specimen is dried in alcohol or in a drying chamber overnight at 30 – 40 °C.

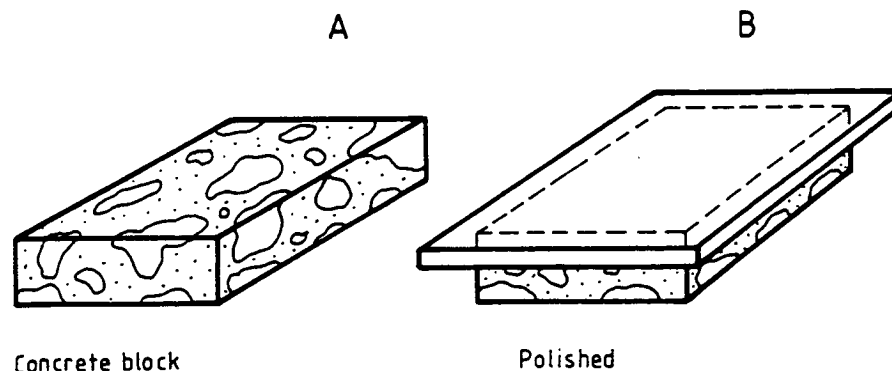


Figure 1 Test sample (A) of concrete, glued on a microscope slide (working glass) and face ground (B).

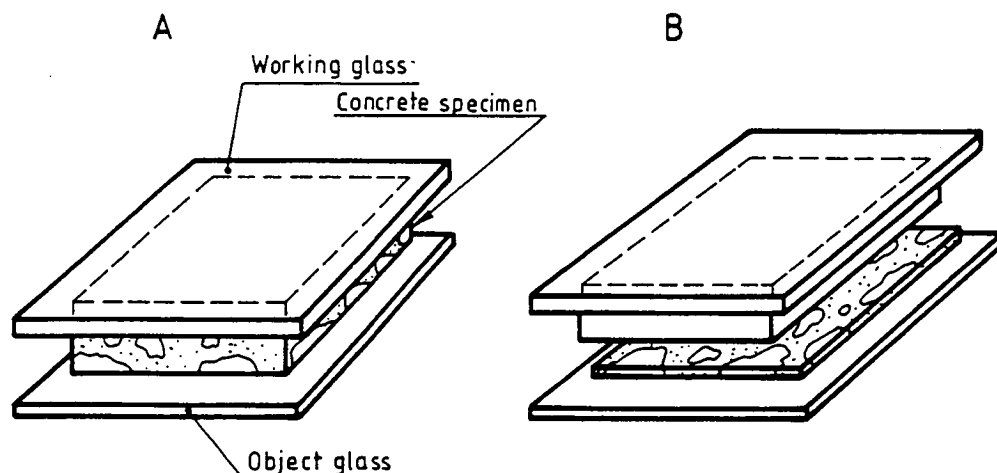


Figure 2 The impregnated sample mounted on a microscope slide (object glass) (A) and cut approximately 1 mm above the object glass (B)

Impregnation

The specimen is evacuated in a vacuum chamber at maximum 0.05 Bar for approximately 10 min. The epoxy, prepared in advance, is added and the vacuum is maintained for another 10 minutes. The specimen is then stored in a plastic bag at normal atmosphere until the hardening of the epoxy is complete.

Grinding of the lower surface of the thin section

The specimen is ground until the edges of the air voids are sharp. The paste should, however, still be fully impregnated with epoxy. To ensure that the surface is satisfactory, grinding should be carried out in two steps. First there should be face grinding to achieve an absolutely plane surface, followed by final grinding on the grinding disc to achieve a smooth surface.

Mounting on microscope slides

The specimen is glued to a microscope object glass slide with the ground face towards the slide, see figure 2.

Grinding of the upper surface of the thin section

The specimen is cut approximately 1 mm above the glass slide, see figure 2.

The upper surface of the thin section is face ground on the face grinding machine until the thickness of the specimen is about 0.05 mm. Grinding is then continued on the grinding disc until the thickness is 0.025 mm. The thickness is checked by use of birefringent colours of common minerals such as quartz and feldspar.

It is very important that the thickness is the same in all parts of the thin section.

Finishing the thin section

The cover glass is mounted on the specimen with Canada balsam, see figure 3.

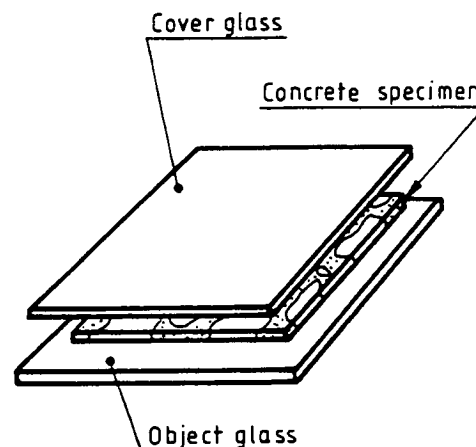


Figure 3 The concrete slice on the object glass is ground to a thickness of 25 microns and protected with a cover glass.

6.3.2 Thin section of the reference concrete

Six different batches of concrete are made.

Concrete for making reference samples should have the following composition

W/C ratio	0.35; 0.40; 0.45; 0.5; 0.6; 0.7
Maximum size of aggregate	8 mm
Paste content	~ 30 % by volume

Slump 60 – 80 mm

Air content ~ 3 %

Plasticizer if necessary

From each batch of concrete a sample is prepared according to NT BUILD 201. Thin sections from each reference sample are then prepared according to section 6.3.1. The thin sections used as references should always be stored in a dark place.

New references should be prepared when the method for sample preparation is changed.

Once a year the intensity fluorescence of the reference samples should be checked. If there have been any changes new reference samples must be made.

6.3.3 Thin section of test samples

A thin section of the test sample is made according to section 6.3.1 and in the same way as the reference samples are prepared.

The following should be noted:

- The paste content and air void content must be of the same order as in the reference samples
- The thickness of the thin sections of the test sample and of the reference samples must be 25 microns.

6.4 Procedure

6.4.1 Examination of test samples

The exciter filter and the barrier filter are placed in the ray path of the microscope. The test sample is placed on the microscope stage. The reference samples are then placed on the stage by turn. The W/C ratio is determined to the nearest 0.05 by comparing the fluorescent intensity of the samples.

The W/C ratio is determined in 10 different fields of images.

The range of variation between the fields is calculated.

During the examination the following must be considered:

- The air void content and the cement paste content in the field of image of the test sample and the reference sample must be of the same order.
- Each field of image must be in uncarbonated cement paste and at least 5 mm from the original surface of the concrete.

6.5 Results

The W/C ratio is determined as the mean value of the W/C ratio in 10 fields of images.

The W/C ratio is stated as a non-dimensional number with two decimals where the second decimal is rounded to 0 or 5.

The variation of the W/C ratio is stated as homogeneous, inhomogeneous or very inhomogeneous, according to table 1.

Table 1 Homogeneity of cement paste

Homogeneity	Range of variation of W/C in 10 fields of images
Homogeneous	< 0.1
Inhomogeneous	0.1 – 0.2
Very inhomogeneous	≥ 0.2

6.6 Test report

The test report shall include the following information, when relevant:

- a) Name and address of the testing laboratory
- b) Identification number of the test report
- c) Name and address of the organization or the person ordering the test
- d) Purpose of the test
- e) Method of sampling and other factual information (date and person responsible for sampling)
- f) Name and address of manufacturer or supplier of the tested object
- g) Name or other identification marks of the tested object
- h) Description of the tested object
- i) Date of supply of the tested object
- j) Date of test
- k) Test method
- m) Any deviations from the test method
- n) Test results
- o) Inaccuracy or uncertainty of the test results
- p) Date and signature

Concrete and Structures Advisory Committee

Chairman

James J. Murphy
New York State Department of Transportation (retired)

Vice Chairman

Howard H. Newlon, Jr.
Virginia Transportation Research Council (retired)

Members

Charles J. Arnold
Michigan Department of Transportation

Donald E. Beuerlein
Koss Construction Co.

Bernard C. Brown
Iowa Department of Transportation

Richard D. Gaynor
National Aggregates Association/National Ready Mixed Concrete Association

Robert J. Girard
Missouri Highway and Transportation Department

David L. Gress
University of New Hampshire

Gary Lee Hoffman
Pennsylvania Department of Transportation

Brian B. Hope
Queens University

Carl E. Locke, Jr.
University of Kansas

Clellon L. Loveall
Tennessee Department of Transportation

David G. Manning
Ontario Ministry of Transportation

Robert G. Packard
Portland Cement Association

James E. Roberts
California Department of Transportation

John M. Scanlon, Jr.
Wiss Janney Elstner Associates

Charles F. Scholer
Purdue University

Lawrence L. Smith
Florida Department of Transportation

John R. Strada
Washington Department of Transportation (retired)

Liaisons

Theodore R. Ferragut
Federal Highway Administration

Crawford F. Jencks
Transportation Research Board

Bryant Mather
USAE Waterways Experiment Station

Thomas J. Pasko, Jr.
Federal Highway Administration

John L. Rice
Federal Aviation Administration

Suneel Vanikar
Federal Highway Administration

11/19/92

Expert Task Group

Amir Hanna
Transportation Research Board

Richard H. Howe
Pennsylvania Department of Transportation (retired)

Stephen Forster
Federal Highway Administration

Rebecca S. McDaniel
Indiana Department of Transportation

Howard H. Newlon, Jr.
Virginia Transportation Research Council (retired)

Celik H. Ozyildirim
Virginia Transportation Research Council

Jan P. Skalny
W.R. Grace and Company (retired)

A. Haleem Tahir
American Association of State Highway and Transportation Officials

Lillian Wakeley
USAE Waterways Experiment Station